AIR FORCE INSTITUTE OF TECHNOLOGY

AIR UNIVERSITY
UNITED STATES AIR FORCE

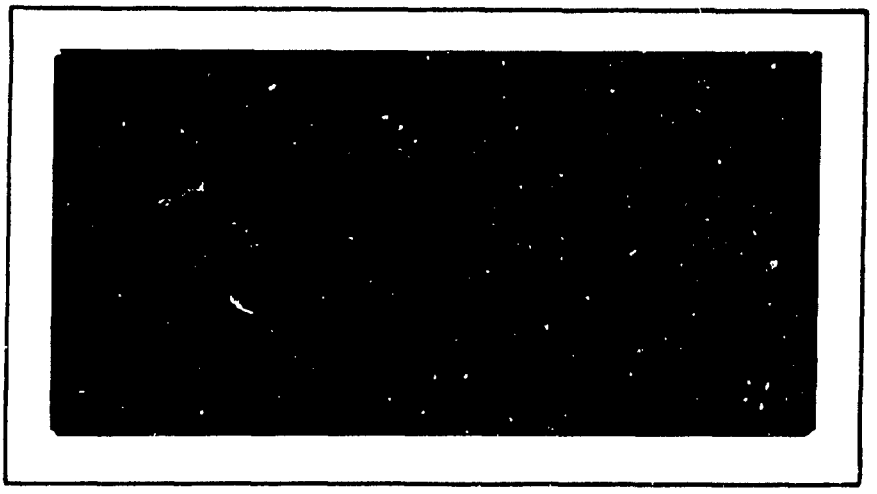

SCHOOL OF ENGINEERING

WRIGHT-PATTERSON AIR FORCE BASE, OHIO

AF-WP-O-SEP 63 3M

CLEARINGHOUSE FOR FEDERAL SCIENTIFIC AND TECHNICAL INFORMATION CFSTI
DOCUMENT MANAGEMENT BRANCH 410.11

LIMITATIONS IN REPRODUCTION QUALITY

ACCESSION # AD 605488

☒ 1. WE REGRET THAT LEGIBILITY OF THIS DOCUMENT IS IN PART UNSATISFACTORY. REPRODUCTION HAS BEEN MADE FROM BEST AVAILABLE COPY.

☐ 2. A PORTION OF THE ORIGINAL DOCUMENT CONTAINS FINE DETAIL WHICH MAY MAKE READING OF PHOTOCOPY DIFFICULT.

☐ 3. THE ORIGINAL DOCUMENT CONTAINS COLOR, BUT DISTRIBUTION COPIES ARE AVAILABLE IN BLACK-AND-WHITE REPRODUCTION ONLY.

☐ 4. THE INITIAL DISTRIBUTION COPIES CONTAIN COLOR WHICH WILL BE SHOWN IN BLACK-AND-WHITE WHEN IT IS NECESSARY TO REPRINT.

☐ 5. LIMITED SUPPLY ON HAND: WHEN EXHAUSTED, DOCUMENT WILL BE AVAILABLE IN MICROFICHE ONLY.

☐ 6. LIMITED SUPPLY ON HAND: WHEN EXHAUSTED DOCUMENT WILL NOT BE AVAILABLE.

☐ 7. DOCUMENT IS AVAILABLE IN MICROFICHE ONLY.

☐ 8. DOCUMENT AVAILABLE ON LOAN FROM CFSTI (TT DOCUMENTS ONLY).

☐ 9.

NBS 9/64 PROCESSOR:

PARTICLE SIZE DETERMINATION BY USE OF ELECTROSTATIC PRECIPITATION PATTERNS AND RADIOACTIVE TRACERS

THESIS

GA/Phys/64-2

Gonzalo Fernandez
Lt Col USAF

PARTICLE SIZE DETERMINATION BY USE OF ELECTROSTATIC PRECIPITATION PATTERNS AND RADIOACTIVE TRACERS

THESIS

Presented to the Faculty of the School of Engineering of the

Institute of Technology

Air University

in Partial Fulfillment of the

Requirements for the Degree of

Master of Science

by

Gonzalo Fernandez, B.S.

Lt Col USAF

Graduate Astronautics

August 1964

Preface

This report is a direct result of a two-fold interest which I developed while at the Air Force Institute of Technology. First, I wanted to renew my interest in the air sampling field, a subject to which I had been previously exposed. Secondly, I wanted to work on an experimental thesis rather than a theoretical one. The problem of verifying the validity limits of an electrostatic precipitator theoretical model which could be used as an air sampler was ideally suited to satisfying my two-fold interest.

After having completed my study, the use of an electrostatic precipitator as an air sampler appeals to me even more. It appears to offer many advantages over the sampling equipment of today. I hope that the results which I have obtained will be another step towards the eventual design of a practical electrostatic precipitator air sampler. Through these pages, too, I also hope to pass on to those that follow a little of the enthusiasm which I have felt for this experimental work.

Many people made helpful contributions to my work. The most significant, of course, was from Dr. C. J. Bridgman, my thesis adviser, who spent many hours helping me chart and stay on the course to the ultimate goal. His dynamic interest and unflagging enthusiasm provided great incentive during the entire study, but particularly during those periods in experimental work when nothing seems to go right. For all his efforts, my heartfelt thanks. I would also like to express my appreciation to Dr. Bridgman for his encouraging and helping me present two papers on this work before meetings of the American Nuclear Society. I am also indebted to the men of the Physics Laboratory, who gave of their time and knowledge to help this experiment. To Jim Miskimen, Bob Hendricks, Don Ellworth,

Earl Vance, S/Sgt Bob Bryant, and A/2C Clark Dekoeyer go my sincere thanks.

I should also like to thank Frank Jarvis, John Parks, and Bill Baker of the Mechanical Engineering Laboratory. Their cooperation and assistance at all times was quite helpful in the timely completion of the experimental equipment. My thanks also to Cliff Howell, Technical Photo, Aeronautical Systems Division, for his excellent microphotographic motion pictures; to Mr. M. W. Wolfe of the Air Force Institute of Technology School Shops; and to Major D. E. Dye, Aeronautical Research Laboratory, for all the equipment I borrowed.

Lastly, I must express my appreciation to my wife for having had to become an unwilling expert on children's movies during the last year. Without her able assistance and quiet inspiration this work would certainly not have been possible. My love and admiration go out to her.

Gonzalo Fernandez

Contents

List of Tables

List of Figures

Abstract

The purpose of this thesis is to determine the validity limits of a previously derived theoretical model of an electrostatic precipitator air sampler. The theoretical model is investigated by insertion of radioactive micron-size microspheres into a closed-loop wind tunnel, whose airstream flows into an electrostatic precipitator. The precipitation pattern on the collection plates is determined by the pattern of radioactivity. Ideally, the particles should be segregated by size. The results are compared to the theoretical predictions which are calculated with a digital computer program.

Fourteen runs were made with the 7 ± 3 and 35 ± 5 micron particles using the Scandium-46 isotope. The results indicate good reproducibility and fair overall correspondence between experimental and theoretical data at 750 cm/sec for the 7 ± 3 micron particle and 450 cm/sec for the 35 ± 5 micron particle. However, the experimental and theoretical results tend to diverge as the particle velocity is increased by 200 cm/sec or the applied voltage is decreased in steps of 5 KV and 2.5 KV.

Conclusions are that (1) the results are reproducible within experimental error; (2) the physical phenomena in the precipitator can be described by mathematical models as suggested in the original theoretical study; (3) mathematical models being used are probably imperfect; and (4) investigation of the validity of the theoretical model should continue.

PARTICLE SIZE DETERMINATION BY USE OF ELECTROSTATIC PRECIPITATION PATTERNS AND RADIOACTIVE TRACERS

I. Introduction

General

This thesis is a report of the experimental results obtained in using an electrostatic precipitator for determining sizes of radioactive particles in the range of 4 to 40 micron diameter. Results of previous theoretical studies were used as the basis for the experiment, which simulated collection of atmospheric particles by an electrostatic precipitator air sampler. Particles of known size and known radioactivity were injected into a closed-loop wind tunnel, which had an airstream of known velocity flowing through a three-plate, two-stage electrostatic precipitator. The precipitation pattern of the collected particles was determined by the pattern of radioactivity on the collection plates. The experimental deposition pattern was compared with the pattern theoretically predicted by a digital computer program which was based on the original theoretical study.

The need and desirability of an efficient air sampler based on large volumes of air sampled has been discussed and established by Lamberson (Ref 6), Baker (Ref 1), and Chiota (Ref 2). A sampler based on principles of electrostatic precipitation could theoretically determine particle sizes and the corresponding radioactivity thereof. The usefulness of such an efficient device near a nuclear detonation,

as an airborne sampler, or even as a stationary monitor needs no elaboration. This study is a direct effort to experimentally determine the limits of validity of the theoretical model previously developed, in order that the model might serve as the basis for a spectral collector design.

However, for a clear understanding of the work covered in this thesis, it is essential that the principle of electrostatic precipitation be understood and that the previous studies completed on this subject at the Air Force Institute of Technology be briefly reviewed. To this end, the remainder of this introductory chapter will be devoted to covering the principles of electrostatic precipitation and to the previous research done in this area. Discussion in detail of the original theoretical study by Captain Donald L. Lamberson (Ref 6) will be deferred until Chapter II, where it will be included as background to the statement of the problem. A description of the experimental apparatus will follow in Chapter III. In Chapter IV, the experimental procedures will be described. The results obtained and their analysis will be the subject of Chapter V. Conclusions and recommendations for future action will be in the final chapter, Chapter VI.

Electrostatic Precipitation

The principles of electrostatic precipitation as used in this experiment have been known for years and are widely applied in industrial uses. These principles are thoroughly covered and excellently discussed by both Lamberson (Ref 6: Chaps III & IV) and Baker (Ref 1:10-24). It is, therefore, not the intent here to either duplicate or extend on their discussions, but rather to cover only those portions deemed essential to understanding of the current research.

The basic principle of electrostatic precipitation is simply illustrated in Figure 1 by a two-stage precipitator, i.e., a precipitator having separate charging and collection sections. The first stage contains a charging grid, usually made of fine wire wrapped around a frame. As the potential difference between the grid and the opposite plate is increased to the point where the air becomes ionized, a current begins to flow. The grid acts as the current source. This current is called corona current, or corona discharge. The second stage contains the collection plates, which although maintained at a high potential difference, do not have any current flow. The collection plates are at ground potential, while the grid and center plate are at a high negative potential. The corona current produced by this combination is known as "negative" corona.

Referring to Figure 1 again, it can be seen that the air bearing the aerosol is forced between the plates at the left end by some type of pumping device. On entering the precipitator, the air flows by the charging grid in the first stage. It is in this section that the particles become negatively charged through absorption of electrostatic charge. The magnitude of the absorbed charge, according to Lamberson is dependent upon the current density in the corona field, the size of the particle, and amount of time spent in the charging section (Ref 6:38-39). After leaving the charging section, the charged particles move into the electrostatic force field of the collection section, where their trajectory is now defined by two components, i.e., the particle linear velocity and the transverse velocity generated by the coulombic charge differential.

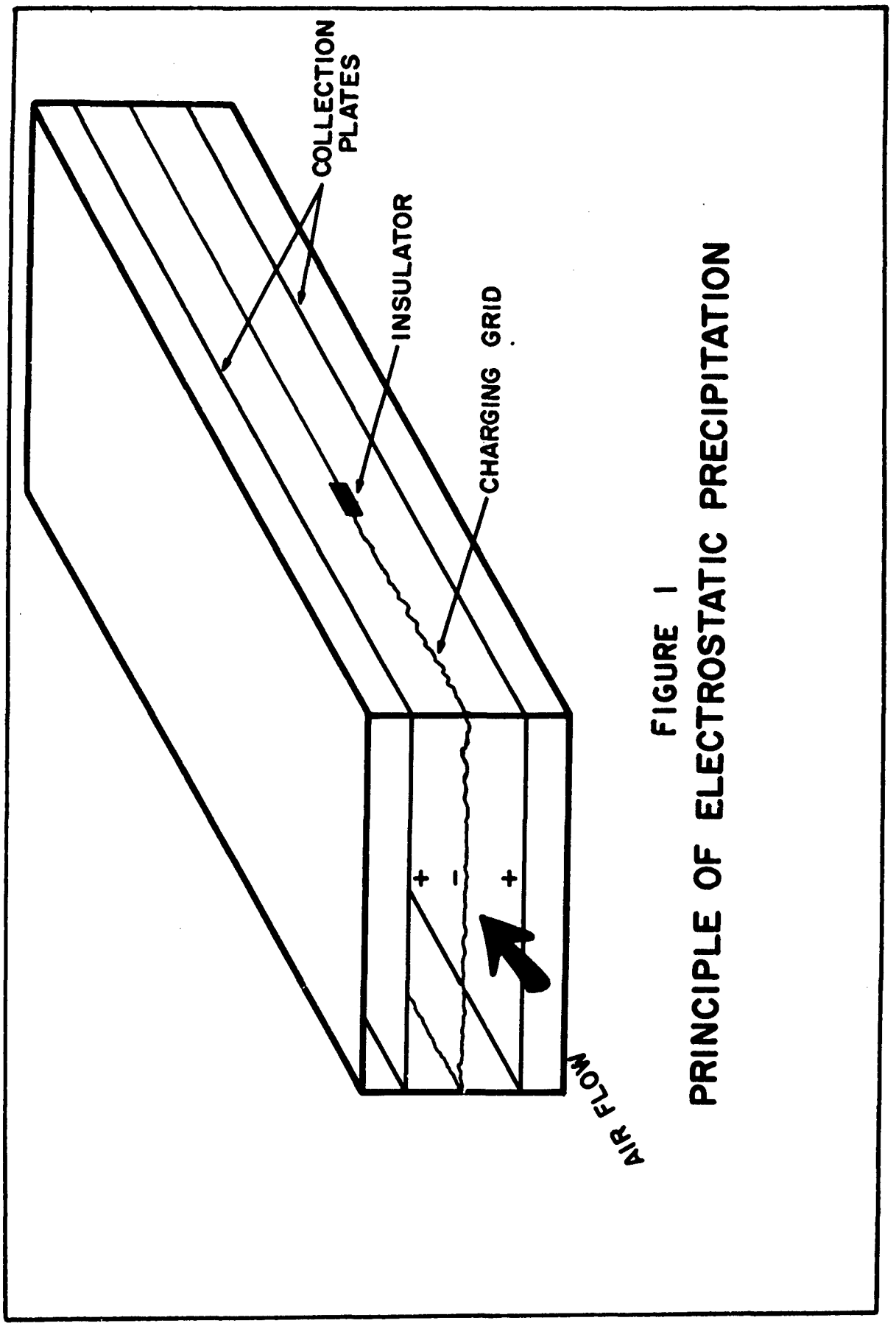

FIGURE 1
PRINCIPLE OF ELECTROSTATIC PRECIPITATION

Charging Mechanisms. As pointed out by Lamberson "negative" corona has proven the most efficient charging medium for use in electrostatic precipitation work (Ref 6:29) and was the type used in this study. The technical description of corona given by Lamberson is of interest as background to the manner in which particles acquire their charge. Two separate mechanisms have been found responsible for the charging which occurs in the corona discharge area. The processes are bombardment charging and diffusion charging. Bombardment charging results when a particle is struck by an ion whose motion is along the lines of the corona electric field. Diffusion charging, on the other hand, results from the attachment of an ion which is in random motion relative to the particle. Bombardment charging predominates for particles .3 micron radius and larger while diffusion charging predominates for particles less than 0.1 micron radius (Ref 6:40-42). The charge thus acquired by a particle traversing a corona field, either by bombardment or diffusion charging, can be described by non-linear differential equations. However, since the radioactive particles used in this study were greater than 1.0 micron radius, the diffusion charging process did not apply and will not be further considered.

Particle Behavior. A particle entering the corona discharge area with a linear velocity will become charged by the mechanisms described above (See Fig. 2). As the charged particles travel through the electrostatic field in both the charging and collection sections, the field exerts a force transverse to the air flow and generates a transverse, or drift, velocity. As given by Lamberson, this velocity will acquire a terminal value practically instantaneously and can be described mathematically by Stokes' law (Ref 6:51). Since all the

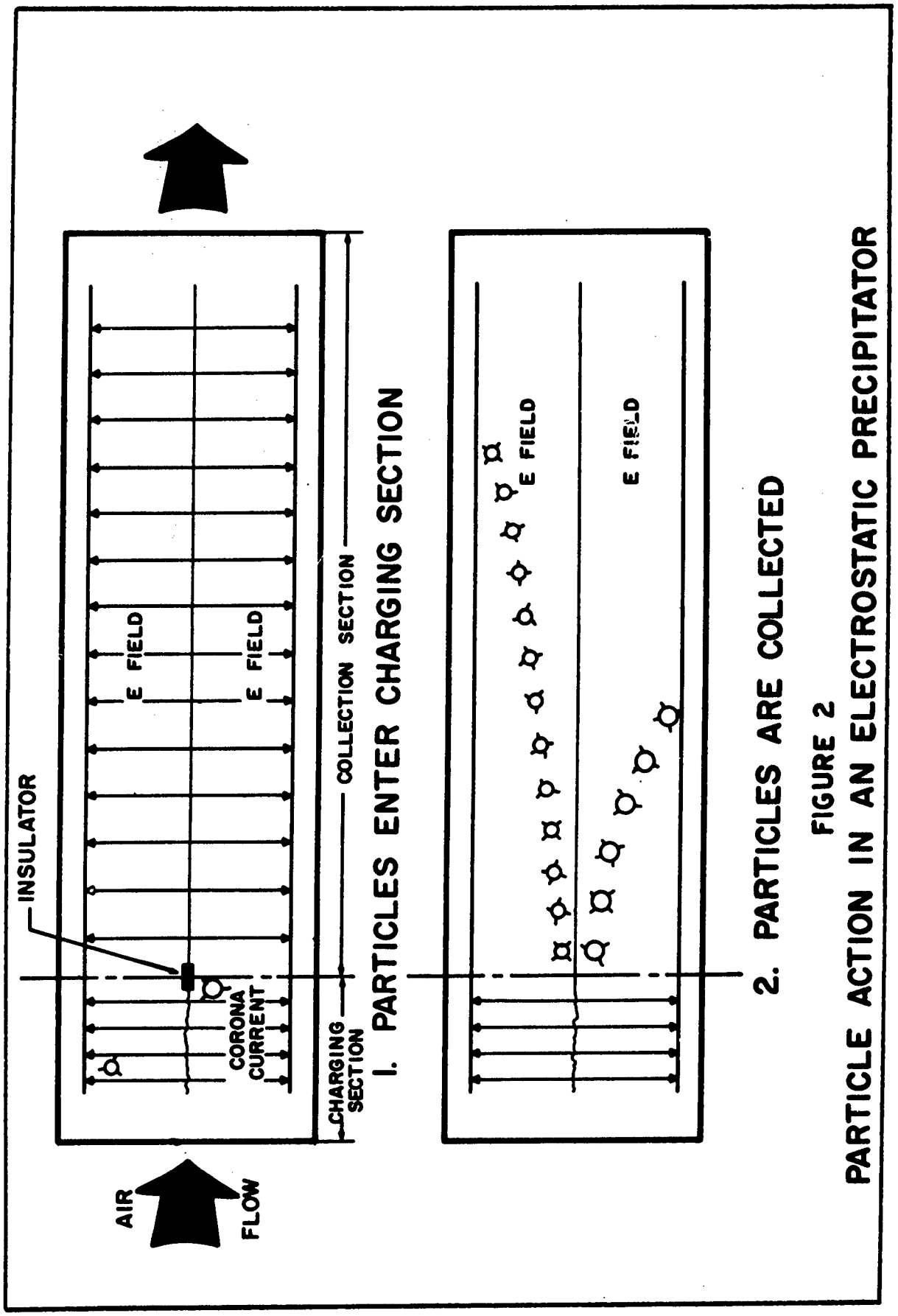

FIGURE 2
PARTICLE ACTION IN AN ELECTROSTATIC PRECIPITATOR

physical phenomena involved can be described by mathematical equations, it is possible to predict whether the particle will be collected within the precipitator or not. In other words, if the transverse, or drift, velocity divided by the plate separation distance is equal to or less than the linear velocity divided by the plate length, the particle should strike the plate and be collected. It was this principle of electrostatic precipitation that Lamberson used in his theoretical approach to an electrostatic precipitator air sampler.

Previous Research

Lamberson (Ref 6) completed the original theoretical study proposing the electrostatic precipitator as an air-sampling, particle-sizing device during the 1961 academic year. Since then several theses based on his study have been completed. The first thesis was a feasibility study completed by Baker during the 1962 academic year. For his study, Baker built an experimental precipitator (EARC-I), which contained seventeen plates in the collection section (nine plates at ground potential and eight at a high, variable, negative potential of up to 18.5 KV) and eight charging grids. With this apparatus, it was possible to sample large volumes of air (flow rates were approximately 45 m^3/min) from which atmospheric radioactive samples were actually collected. This proof-test of using a precipitator as an air sampler, however, involved a rather lengthy and tedious method of extracting the samples from the plates and compacting them into an analyzable quantity (Ref 1:Chaps IV and VI).

Concurrently with Baker's experimental work, Stuart developed a digital computer program for theoretically analyzing the performance

of an electrostatic precipitator. Using the operating parameters of Baker's EARC-I precipitator, Stuart presented an analysis of the experimental precipitator as well as an optimization of a two-stage, parallel-plate precipitator. Stuart further presented a proposed design for a small, airborne precipitator, which could be built and tested in a high-speed wind tunnel (Ref 7:Chap VI). This precipitator design has not yet been constructed.

During the following academic year, 1963, Chiota attempted to correlate the particle size distribution collected experimentally by the EARC-I with a predicted theoretical distribution based on Lamberson's work. However, because the particles were counted by use of a microscope and because some of the variables could not be controlled, the results achieved by the study appear to be inconclusive (Ref 2).

From examination of the previous research, it was clear that the original theoretical work had never been subjected to rigorous experimental verification. The experimental work subsequent to Lamberson indicated that the use of an electrostatic precipitator as an air sampler was feasible; therefore, it was felt that the basic theory should be thoroughly tested before any further design work was done. The present study is the first step in a rigorous experimental verification of the theoretical conclusions presented by Lamberson. Defining this first step as an experimental problem is done in the next chapter, Statement of the Problem.

II. Statement of the Problem

From the basic principles of electrostatic precipitation given in Chapter I, it is evident that this phenomenon possesses an ability to collect different-size particles at different stations along the axial direction of the airflow. Lamberson used this principle as a basis for predicting the mass fractions of various-sized atmospheric aerosols that could be collected by the electrostatic precipitator air sampler - a sampler that would have a much higher sensitivity than those in use today. This chapter briefly discusses the theoretical basis of Lamberson's argument as a background to reducing the verification problem to an experimental one.

Theoretical Basis

A differential equation derived by White (Ref 11) describes the charging of particles by bombardment. Combining this equation with the physical laws applying to particle behavior, Lamberson developed the concept for his theoretical model. Several assumptions also played an important part not only in the solution of the charging problem but in the development of the theoretical model as well.

Assumptions. Three assumptions were considered necessary by White to solve the bombardment charging problem. He lists them as (Ref 11:1187):

1. The aerosol particles are spherical.
2. Particle diameter is much less than distance between particles.
3. In the immediate region surrounding a particle, the ion concentration and electric field are uniform.

These assumptions were also considered in defining the verification problem and their applicability (or lack of it) during the experimental runs probably had a great influence in the results achieved. This item will be further discussed with the results in Chapter V.

Bombardment Charging. Using the assumptions listed, White derived a differential equation for bombardment charging. Lamberson took White's equation and, by assuming that the dielectric constant, K, of atmospheric aerosols was 4, developed it into the following form (Ref 6:43):

$$\frac{dq}{dt} = A - Bq + Cq^2 \qquad (1)$$

where $A = 11.16\ GR^2E$

$B = 1.61 \times 10^{-6} G$

$C = 5.79 \times 10^{-14} \frac{G}{R^2E}$

q = Particle charge (electrons)

G = Ion density $\frac{\text{ions}}{\text{cm}^3} = 0.352 \times 10^{19} \frac{CUR}{(E)(AREA)}$

R = Particle radius (cm)

E = Electric field $\frac{\text{volts}}{\text{cm}}$

CUR = Corona current (amperes)

$AREA$ = Cathode area (cm^2)

The value assumed by Lamberson for the dielectric constant, K, of atmospheric aerosols was a gross average based on an extensive literature search (Ref 6:21-22). (The same value, 4, was used in the current study because the commercial producer of the radioactive

microspheres, could not provide the author with the exact composition of the particles. The composition apparently falls under company proprietary rights. The lack of time precluded an experimental determination of the K value).

Other Assumptions. In arriving at the mass fraction of atmospheric aerosol particles that an electrostatic precipitator could theoretically collect, Lamberson made other significant assumptions. First, he divided the aerosol distribution spectrum into twelve arbitrary groups. Since the table of these groups is available in the four previous studies and the division, as such, is not pertinent to the present study, it is not reproduced here. His second assumption was that the atmospheric aerosol distribution spectrum under consideration is the mean distribution spectrum of long-lived fission products of stratospheric origin. In other words, the radioactivity fraction in a group equals the volume fraction of the same group, which also equals the mass fraction of that group (assuming constant density). The third assumption was that the lower and upper limits of the distribution spectrum for long-lived fission products are 0.1 and 10 micron radii, respectively (Ref 6:64). the last assumption was the general guide in choosing particle sizes for the current study.

Collection Mechanism. Lamberson applied Stokes' law to small, spherical particles traveling in an electrostatic force field in order to determine the drift, or transverse, velocity that a particle acquires relative to the airstream. Where applicable, the Cunningham Correction was used. As a result, the drift velocity in the charging section for air at 75°F and 1 atm may be expressed as (Ref 6:67-72; 8:13-15):

$$V_D = 4.73 \times 10^{-10} \frac{(Q)(E)\ CUN}{R} \qquad (2)$$

where V_D = Drift velocity at any instant (cm/sec)

Q = The charge achieved by the particle at that instant of time in electrons

CUN = The Cunningham Correction to Stokes' law for a particle of radius R or,

$$= 1 + \frac{9.42 \times 10^{-6}}{R} (1.23 + 0.41e^{-.934 \times 10^{5}R})$$

R = Radius of particle or particle group (cm)

In the collection section, there is no charging and the drift velocity is a terminal value based on the total charge acquired in the charging section. This expression, very similar to equation (2), is (Ref 6:72-77; 8:16-19)

$$V_O = 4.73 \times 10^{-10} \frac{(QQ)\ (ECOL)\ CUN}{R} \qquad (3)$$

where V_O = Terminal drift velocity in the collection section for air at 75°F and 1 atm

QQ = Total charge achieved in charging section, a constant (electrons)

$ECOL$ = Voltage in the collection section (Volts)

CUN and R are as defined in (2)

As pointed out earlier, if the time spent by the particle in the precipitator, i.e., the particle linear velocity divided by precipitator plate length, is equal to, or greater than, the time of travel between the collection plates, i.e., drift velocity divided by the plate

separation distance, the particle will strike the collection plate and be collected. Using the drift velocities as well as the assumptions listed under "Other Assumptions", Lamberson theoretically determined the mass fraction of particles which would be collected in a paralle plate precipitator from each of his arbitrarily-determined groups. He further demonstrated that, theoretically, a precipitator of high sensitivity and fair efficiency was possible.

Extension of Theory. By a simple extension of the theory developed by Lamberson, it can be seen that if the linear and drift velocities of a particle in a precipitator are known (or can be accurately predicted), the resultant velocity and trajectory of the particle can be computed. Thus, if the trajectory is known, the point at which the particle will strike the collection plate and be collected can be predicted. This, then, became the basic premise in experimentally verifying the theoretical basis of an electrostatic precipitator air sampler.

Definition of the Problem

In defining the verification problem, it is well to briefly restate some of the factors used by Lamberson. The first factor is that the charge acquired by a particle in a precipitator is, among other things, dependent on its size. The second factor is the assumption that the fission product radioactivity fraction within an aerosol group is equal to the volume fraction of the same group, which in turn is equal to the mass fraction of the group (assuming constant density). In other words, the radioactivity is assumed to be proportional to the particle volume also.

Keeping the two factors in mind, one method of attacking the problem becomes clear. For example, suppose that equal numbers of two different size particles were injected into an electrostatic precipitator at the same point and with the same linear velocity. Each of the two particle sizes would acquire a different charge dependent on its size and would be deposited at a different point on the collection plate. Allowing some random variation for velocity, charge acquired, etc., one might expect a Gaussian distribution about these collection points. This is shown schematically in Figure 3. If the radiation is proportional to mass volume, the areas under the curves will be proportional to the total volume (not the number of particles) of the sample of a given size. Further, if the radiation is different for each size group, the two peaks could be separated by radioactive analysis even in the case of severe superposition. As will be seen later, peaks in this study were determined by total activity only.

The Problem. The verification problem as defined, then, consisted of two parts. First, a theoretical deposition pattern for a group of uniform-sized particles had to be determined. This theoretical pattern would necessarily be based on the parameters and assumptions originally proposed by Lamberson. Although this would be a theoretical computation, actual operating parameters of an experimental precipitator and an actual particle group could be used. Secondly, an experimental deposition pattern had to be determined by injecting particles of known

1/2 FRAMES

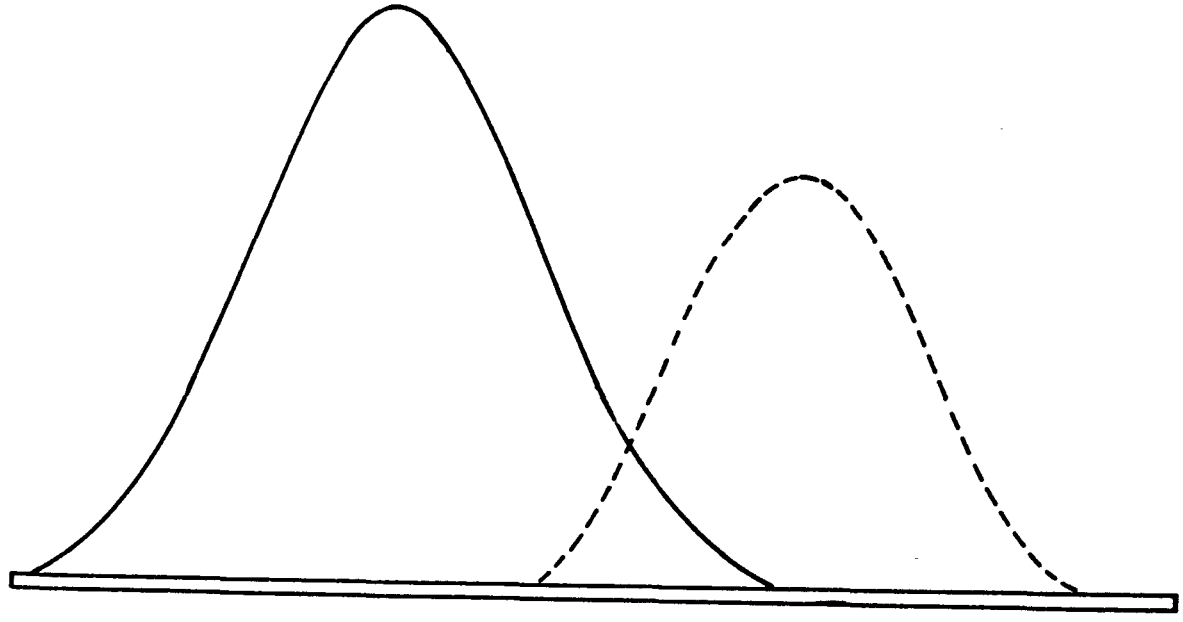

FIGURE 3

IDEALIZED PRECIPITATION PATTERN

15

size and known radioactivity into an airstream with known velocity and which flowed into an electrostatic precipitator. This would simulate collection of a natural aerosol particle group. The operating parameters of the precipitator and particles would be identical for both the theoretical and experimental determinations of precipitation patterns. Comparison of the experimental results with the theoretical predictions should yield the limits of validity of the theoretical model.

In essence, the question that this study sought to answer was: Can the deposition pattern of radioactive aerosols, theoretically predicted based on the parameters of the particle and the electrostatic precipitator, be experimentally confirmed with any degree of certainty and reproducibility?

Objectives. The problem as defined above could be stated as definite experimental objectives. These are listed below.

1. An overall objective of determining the limits of validity of the theoretical electrostatic precipitator air sampler model by comparison of the experimental and theoretically-predicted precipitation patterns.
2. A secondary objective of determining the extent to which the experimental results would be reproducible if all the parameters were held constant.
3. A last objective of determining if and how the precipitation pattern would be affected if the injection position, the particle velocity, or the applied voltage were varied.

Summary

This chapter has dealt with the theoretical basis of an electrostatic precipitator air sampler, which underlies the problem studied in this thesis. Lamberson combined the particle charging equation with the physical laws of particle behavior to develop an air sampler theoretical model. Further, he arbitarily divided the aerosol distribution spectrum into 12 groups and assumed that the radioactivity fraction in an aerosol size group equals the volume fraction of the same group, which also equals the mass fraction of that group (assuming constant density). Another assumption that he made was that the lower and upper limits of the distribution spectrum for long-lived fission products are 0.1 and 10 micron radii, respectively. By extending the theoretical basis, it was shown that the position at which a particle would be deposited along the plate length can be predicted. Injecting particles of known size and known radioactivity into an airstream with known velocity and which flows into an electrostatic precipitator should provide an experimental precipitation pattern which could be compared with a corresponding theoretical prediction. This comparison should yield the validity limits of the theoretical model.

The objectives of the study can be summarized as

1. An overall objective of determining validity limits of the theoretical model by correlation of experimental and theoretical precipitation patterns.
2. The extent to which results can be reproduced.
3. The effect, if any, on the experimental precipitation pattern caused by variation of injection position, particle velocity, or applied voltage.

The apparatus used in achieving the objectives is described in the next chapter.

III. Apparatus

This chapter describes the apparatus used in verifying the theoretical basis of an electrostatic precipitator air sampler. The problem as defined in the previous chapter clearly consisted of a theoretical portion and an experimental portion. This natural division, therefore, was applied in setting up the apparatus for solution of the problem.

Theoretical

For the theoretical portion of the problem, an IBM 7094 Digital Computer was used. The computer program is explained in Appendix A. No further description of this equipment is considered necessary here.

Experimental Apparatus

Overall Description. This paragraph gives an overall description of the experimental apparatus. Further description is given under separate headings of the equipment.

The apparatus utilized for the experimental portion consisted of a closed-loop wind tunnel with an in-line, three-plate electrostatic precipitator and supported by several items of auxiliary equipment. (See Figs. 4 and 5). The major portion of the tunnel consisted of 18" diameter ventilating duct (previously used by Baker) and transition sections leading into and out of the electrostatic precipitator. An 8" x 10" x 24" rectangular wooden duct was used immediately prior to the electrostatic precipitator. It was in this wooden section that the airstream velocity was measured and the injection tube entered the tunnel. A ventilating fan was used as the motive power for the airstream,

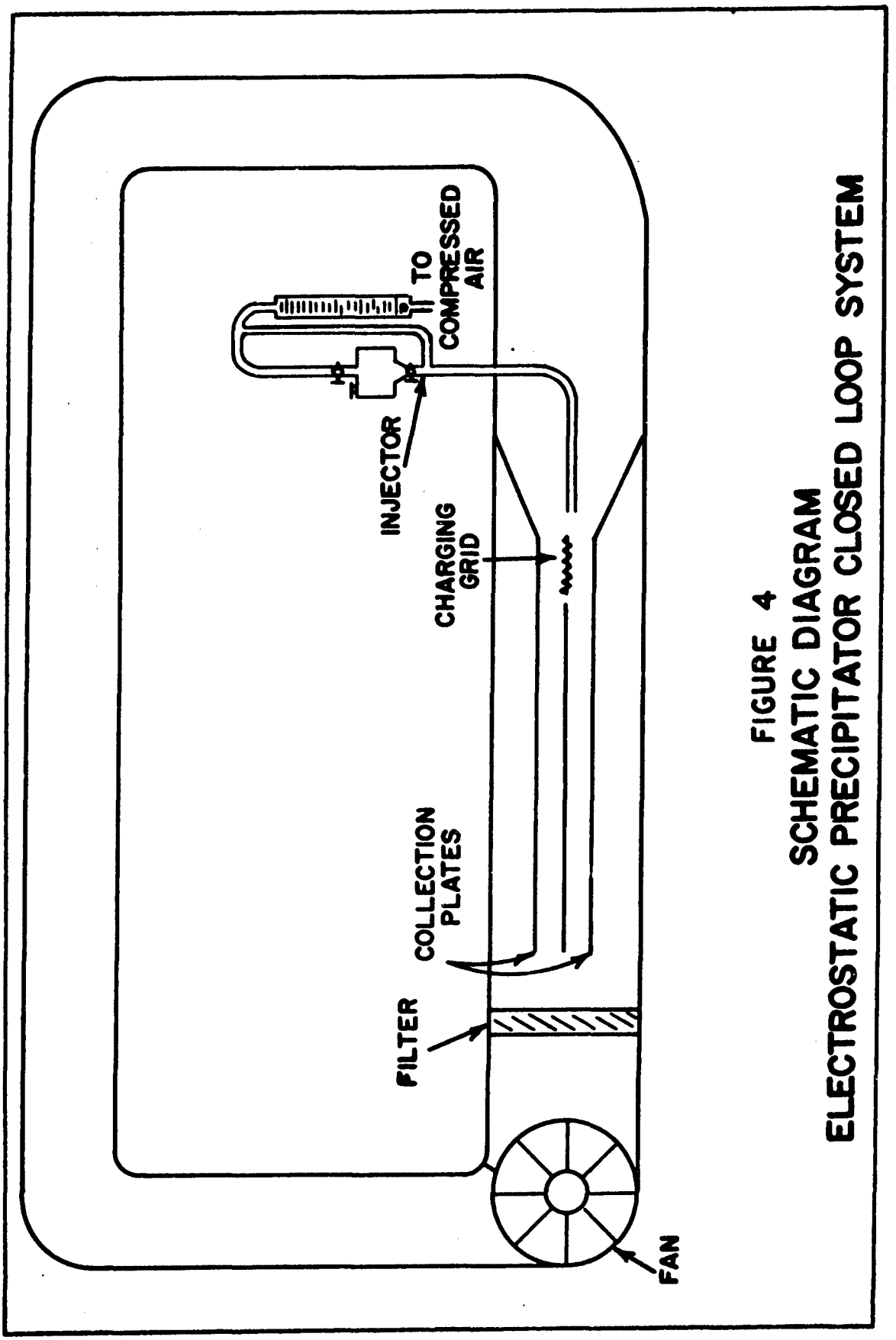

FIGURE 4
SCHEMATIC DIAGRAM
ELECTROSTATIC PRECIPITATOR CLOSED LOOP SYSTEM

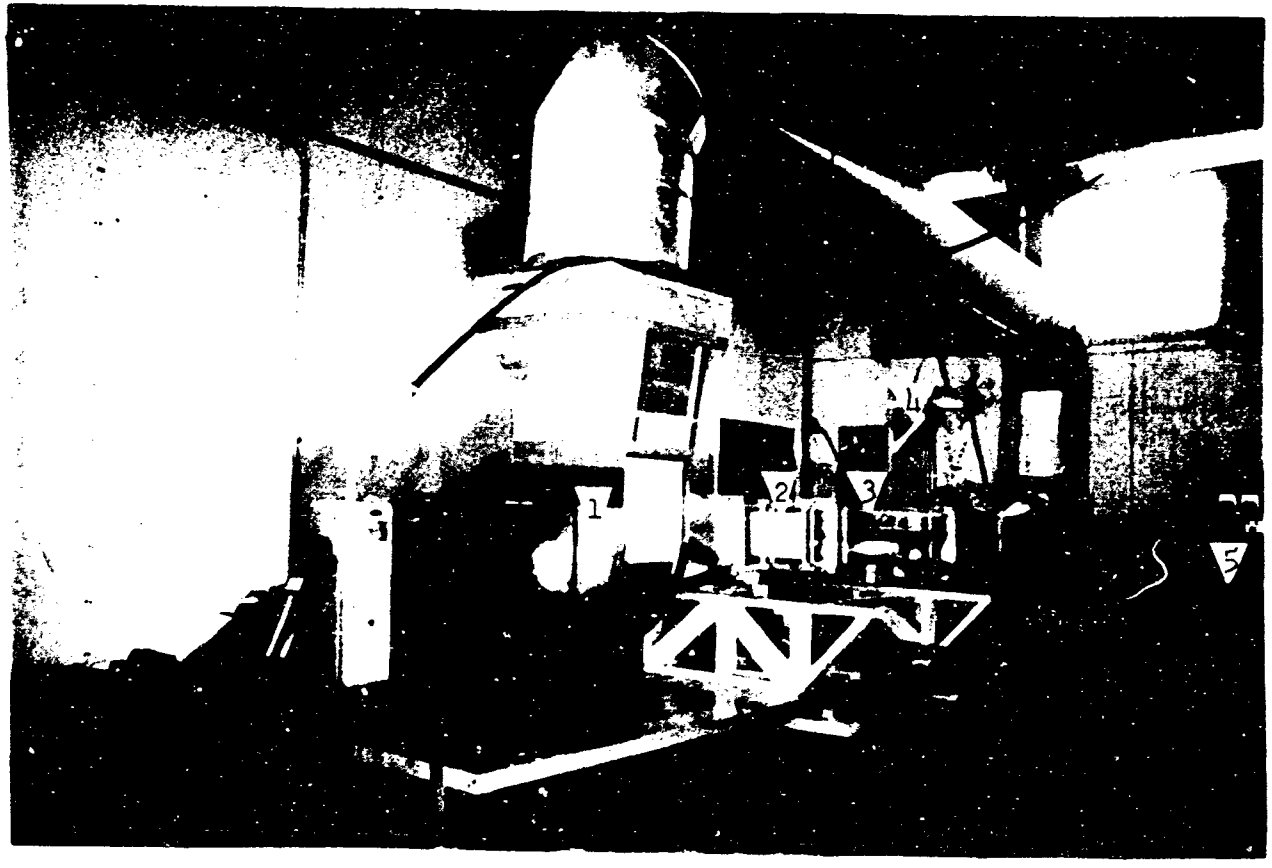

Figure 5
Equipment Room
Wide-angle lens photograph of equipment room showing (1) Fan, (2) Filter, (3) Electrostatic Precipitator, (4) Injection Mechanism, and (5) Hi Voltage Supply.

which was passed through a micron-size mesh, fiber glass filter when exiting the precipitator. The particles were injected by use of compressed air (See Fig. 6). The high voltage required was provided by a DC rectifier.

Electrostatic Precipitator. The electrostatic precipitator, built of 1" plexiglass sides, consisted of two collection plates and one high potential plate. The precipitator inside dimensions were 8" x 10" x 44". The collection plates were 30" polished aluminum plates and were separated by 2 cm from the high voltage plate (also polished aluminum) and the grid. The charging grid consisted of .005" "S" Tungsten wire wrapped around a 6" x 10" polished aluminum frame on 0.25" centers. The frame itself was 0.5" wide on all sides (See Fig. 7). The working side of the precipitator was made as a door, with a piano hinge at the top and four winged nuts securing it at the bottom. The door proved very convenient and quite a time-saver. Except for the number of plates and the door, most of the design features were taken from Baker's design of EARC-I (Ref 1:Chap VI).

Electrical Equipment and Parameters. Utilizing the fact that the air system was to be closed-loop, the electrical circuits were designed with the idea in mind that no large particles or bugs would find their way into the precipitator (one of the items for which Baker was forced to design). An electrical schematic diagram, with the resistor sizes, is shown in Figure 8. Although the light bulb bank used by Baker was kept in the circuit to quench any unexpected surges, its use was never required. The power supply consisted of an NJE Corporation, Model H-30-35, High Voltage Supply, capable of providing negative corona current of 35 ma at 30KV. The corona current which was available as a

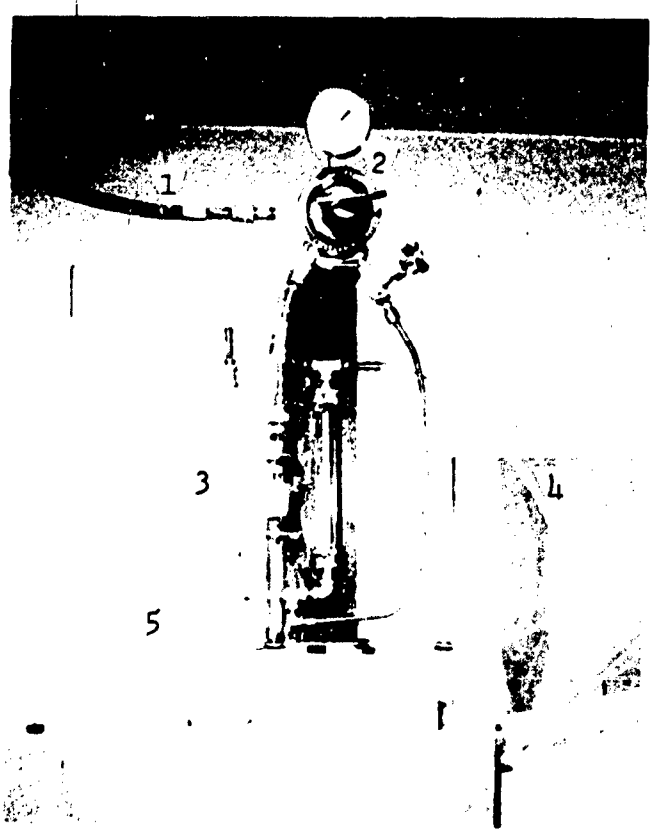

Figure 6
Injection Mechanism
View of Injection Mechanism, showing (1) Compressed Air Line, (2) Regulator, (3) Flow Meters, (4) By-Pass Line, and (5) Injection Tube.

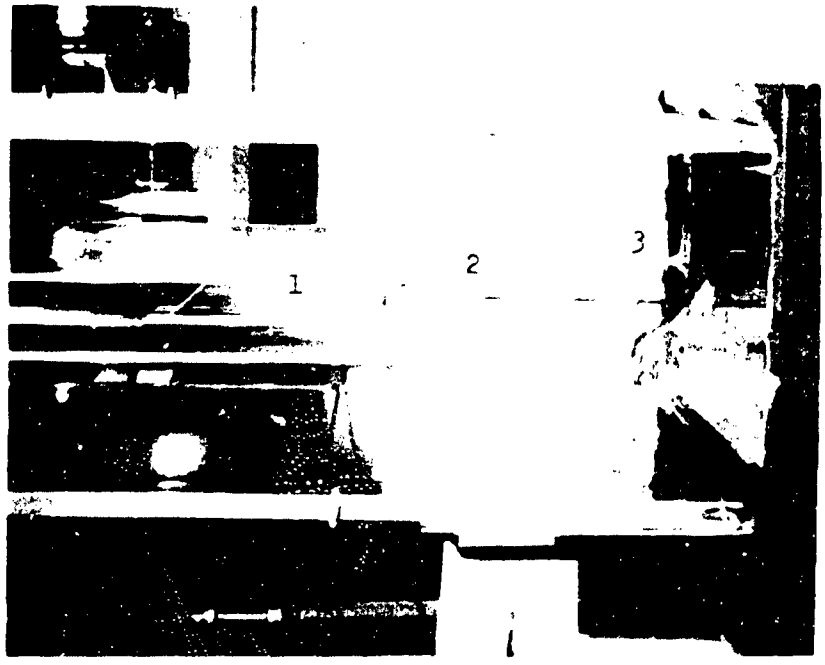

Figure 7
Charging Grid and Injection Nozzle
Closeup view of electrostatic precipitator forward area showing (1) Charging Grid, (2) Injection Nozzle, and (3) Stabilizing Yoke.

1/2 FRAMES

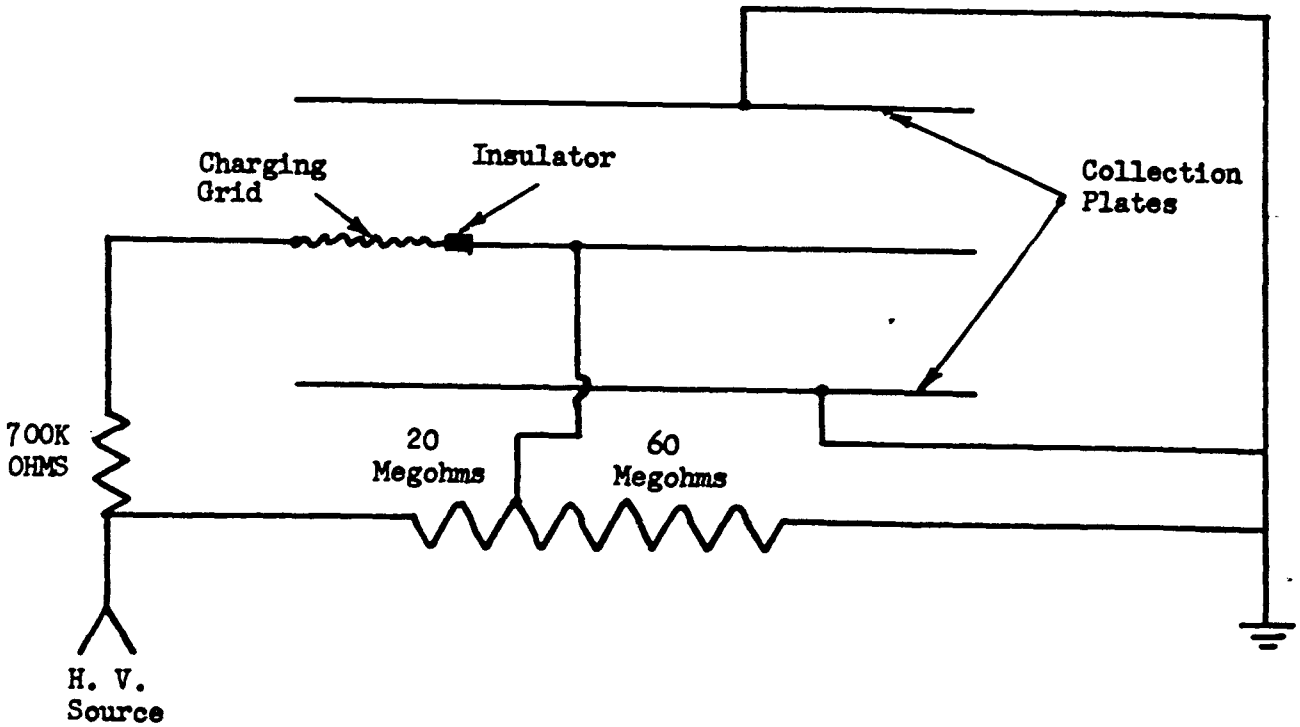

Figure 8
Electrical Schematic Diagram of the Electrostatic Precipitator

function of the applied voltage is shown in Figure 9.

Auxiliary Equipment. The auxiliary equipment for this study included the ventilating fan, the micron-size mesh filter, a hot wire flow meter, high speed cameras, and injection mechanism. The high speed cameras and injection mechanism, however, will be discussed separately.

The ventilating fan was an ILG Electric Ventilating Fan, Model BU 1350, powered by a 1½ HP motor. The filter was a Gelman Company, Type M, fiber-glass filter, rated as 40% efficient against 0.3 micron aerosol. Because the particles used in the study were about an order of magnitude larger, it was felt that two filters in series would provide adequate protection against contamination of the fan or tunnel. Unfortunately, however, the rated capacity of the fan was against a maximum of 2.5" of water static pressure. At the air flows desired, the filters caused a drop of approximately 5" water pressure each (Ref 4:31). It, therefore, became necessary to use only one filter. In the end, air velocities of approximately 500 cm/sec were secured in the test section as against the original goal of 1000 cm/sec and higher. The use of one filter presented no other problems, however, and no contamination was ever found beyond the filter intake side.

The hot-wire flow meter used for measurement of the airstream velocities was a direct-reading Flowtronic Corporation Air Velocity Meter, Model 55A1. The probe of this instrument was inserted through a hole in the wooden tunnel section approximately 18" in front of the electrostatic precipitator. Normal non-compressible air flow relations were used to obtain the velocity of the airflow in the inaccessible, high-voltage precipitator test section.

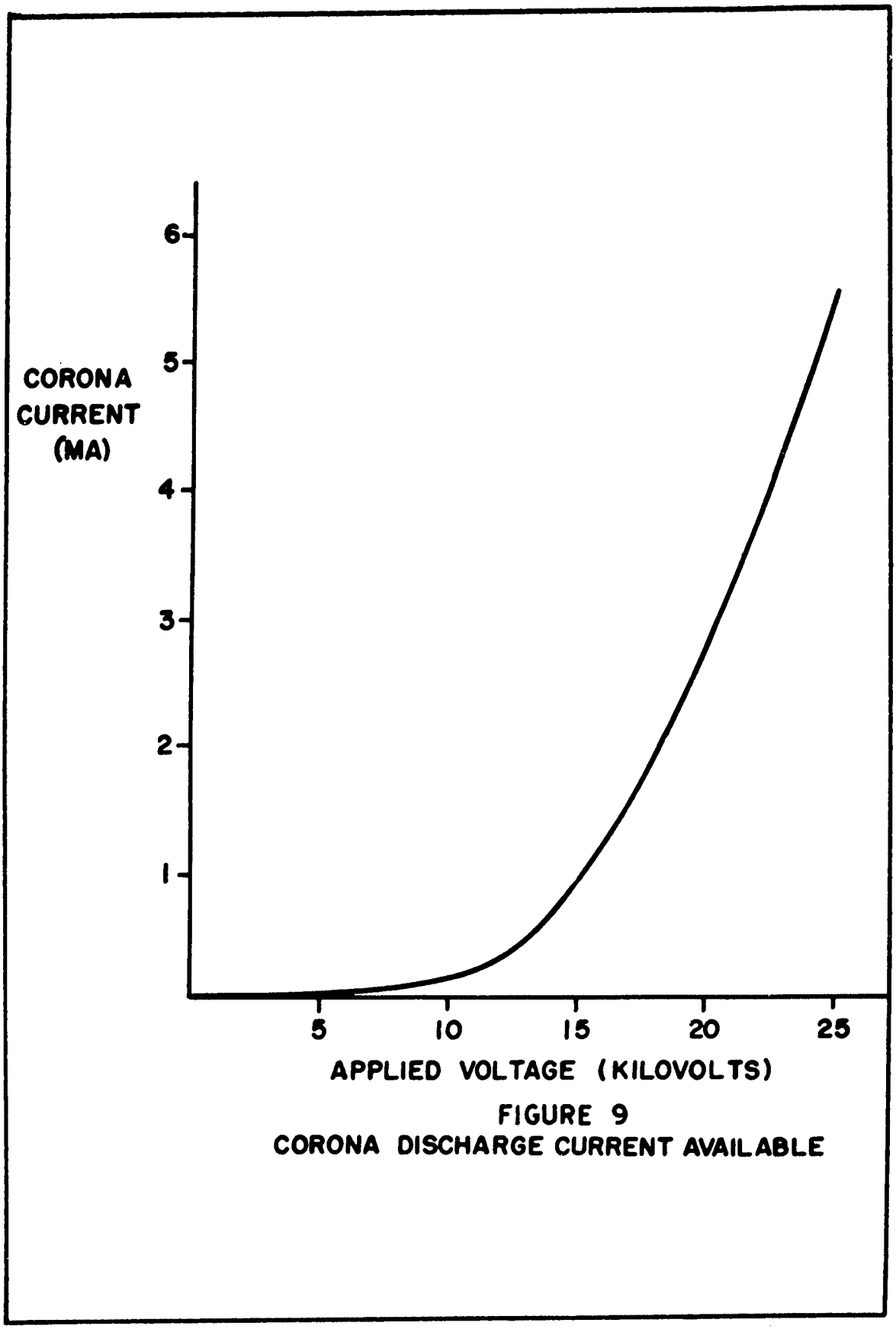

FIGURE 9
CORONA DISCHARGE CURRENT AVAILABLE

Injection Mechanism. The main feature of the injection mechanism was a 1½" radius x 2" long aluminum cylinder with a ¼" hole in the center, threaded at each end to permit insertion of a petcock (See Fig 6). The cylinder, or injector, was in turn connected into the laboratory compressed air line through a regulator with a union above and a tube tee below. These connections made it possible to disconnect the injector so that it could be loaded with radioactive particles inside of a glove box in the radioactive materials room. Keeping both petcocks closed after loading gave assurance that the radioactive particles would be safely contained until the loader was secured in place. Another air line, in parallel with the injector line, led from the regulator through two flowmeters in parallel and rejoined the injector line at the tube tee. (Two flowmeters were used in parallel due to the non-availability of a larger size). Made by RGI (Roger Gilmont Industries), the flowmeters were Size No. 2 with a range of 10-1900 ML/min. The radioactive particles were actually inserted into the main airstream through the tube tee, where the two parallel air lines rejoined. From this point, a flexible 1/8" ID brass tube led into the tunnel and was joined to a 6" stainless steel tube section, .051" inside radius. The stainless steel tube was used as a nozzle because of its rigidity and for its better ejection characteristics at the nozzle end. A four-way yoke attached to the precipitator housing stabilized the steel tube and permitted it to be positioned anywhere in a 2 cm square, i.e., up-and-down or side-to-side (See Fig 7). Compressed air was available from a laboratory line with a maximum capacity of 35psi.

High-Speed Microphotographic Cameras. The microphotography was taken with the Wollensak Fastax Hi-Speed Cameras, capable of speeds of 7000 frames/sec. The frame speed could be doubled by an 8 mm prism adapter, which photographed two 8 mm frames within a 16 mm frame. The lens for photography of the 35±5 micron particles was 6½" with a 6½" extension tube; for the 7±3 micron particles, the same lens with an 8½" extension. The high-speed microphotography made possible the measurement of most of the particle velocities at ejection from the tube nozzle and the determination of particle behavior in the corona and at deposition on the plate. The lens used could not record the 7 micron particle at 950 cm/sec.

Particles

The particles used in the experiment are commercially available, radioactive microspheres produced by the 3M Company Nuclear Products Division. The microspheres are described in a company report as "ceramic bodies of spherical shape and controlled particle size. While the radioisotope itself is bound firmly in the microsphere, the radiation from it can escape and do work. Since these bodies are completely inert physiologically, if ingested by design or accident, they will simply pass through the gastrointestinal tract and be excreted. The radioisotope will not behave in a normal metabolic way, but will be retained by the microsphere, of which it is an integral part (Ref 5:2)." As indicated earlier neither the actual composition of the microspheres nor their dielectric constant is known to the author. The producer of the microspheres did indicate in a personal letter to the author that the compound used as the matrix of the microspheres (after the heat treatment is completed) is a pyrophosphate of a Group 4B ion, i.e., titanim, hafnium, or zirconium.

Scandium-46 was the radioisotope used in the microspheres. The isotope was originally selected on the basis of three factors. First, its half-life of 85-days permitted adequate shipment and working time. Secondly, the isotope emitted two gamma rays on decay (.88 Mev and 1.12 Mev), which would permit use of a scintillation counter for analysis. Lastly, its toxicity level in the insoluble form was considered favorable (Ref 9:29 lists the lung and GI tract as the critical organs with MPC in air of 2×10^{-11} mc/cc and 2×10^{-10} mc/cc, respectively). A Beta ray of .36 Mev is also emitted on the decay of this isotope. In fact, the decay scheme is very similar to that of Cobalt-60, a well known standard in the field (See Fig. 10).

From several sizes available, two different-sized microspheres were selected for the study. The first, selected as an early, "proof-of-principle" type, was a 35 ± 5 micron diameter microsphere with a specific activity of 0.1 mc/gm. The second, selected from the lower range of the available particles, was a 7 ± 3 micron diameter particle with a 50 microcuries/gm specific activity. In addition, inert 35 ± 5 micron microspheres were utilized in preliminary runs to check out the experimental procedures.

Counting Mechanism

The equipment used for the activity measurements consisted of a wooden tray, dolly, Geiger-Muller tube, and a scaler/count rate meter (See Fig. 11). The wooden tray, 80" long x 12½" wide x 1" deep, was lined with aluminum foil and used as a receptable for the collection plates. The dolly, 12" long x 10½" wide, was made of 1" x 1" angle iron with two adjustable 1/8" thick steel plates on the bottom. An adjustable collar, suspended 6" above the dolly center by two steel rods, held the GM tube

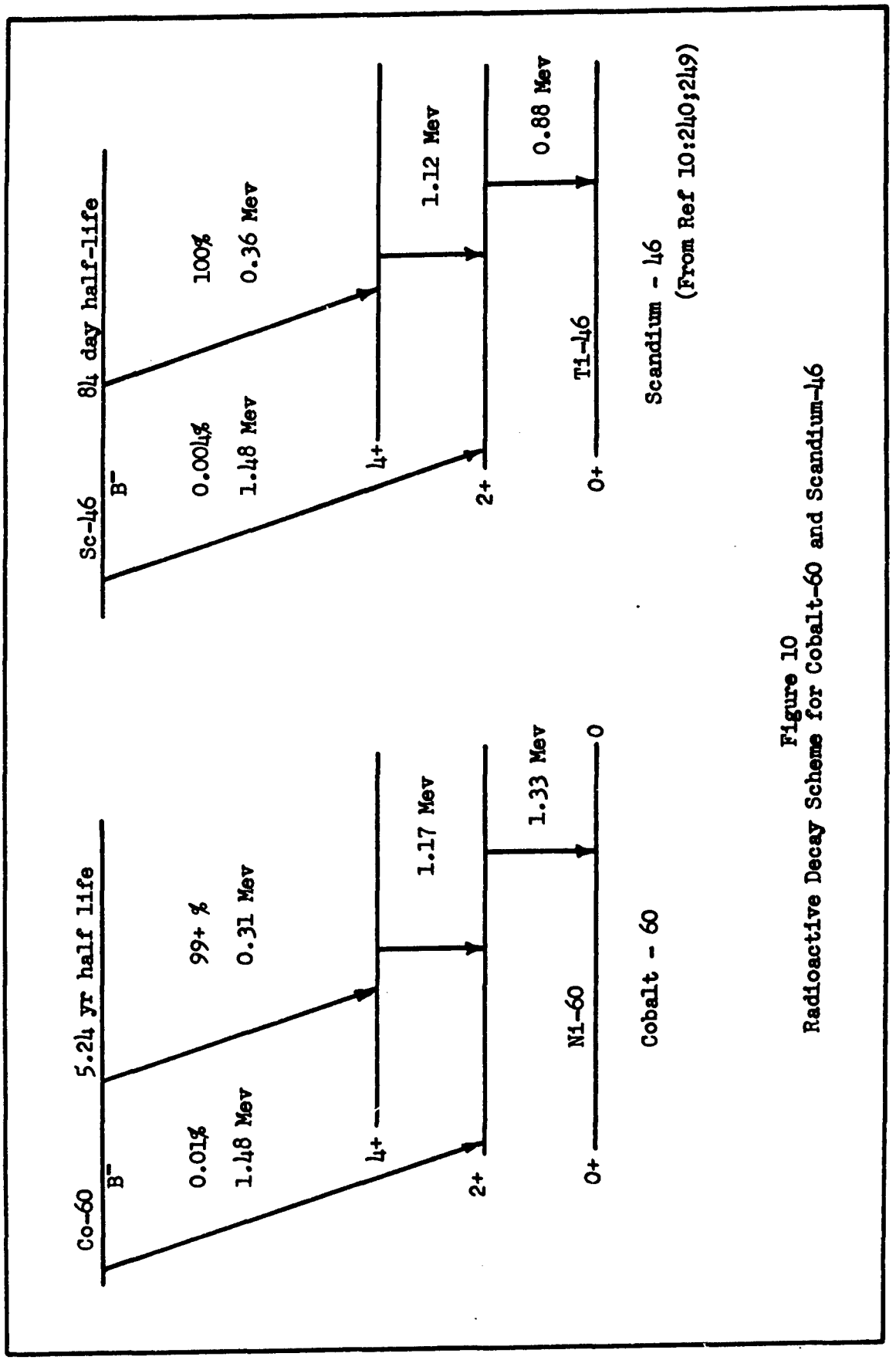

Figure 10
Radioactive Decay Scheme for Cobalt-60 and Scandium-46

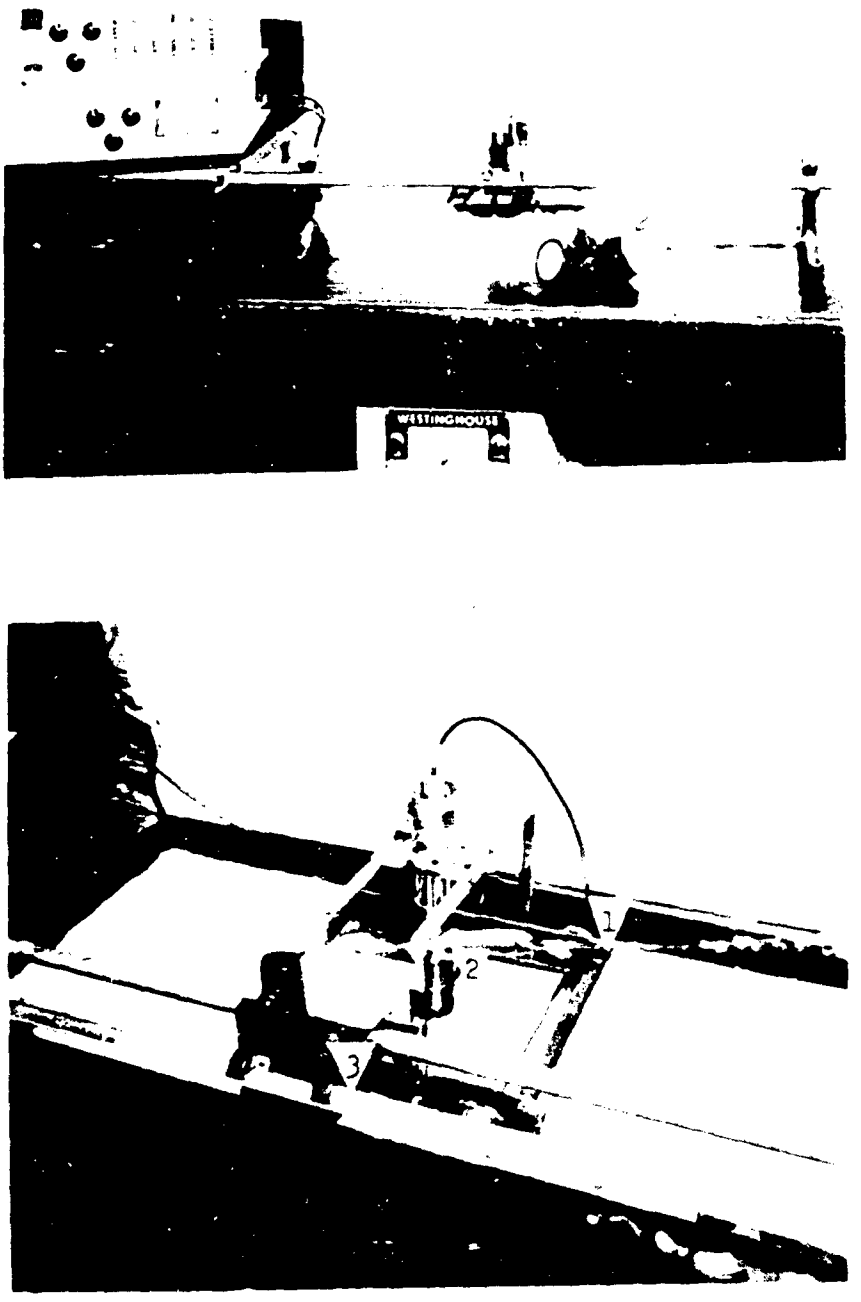

Figure 11
Counting Mechanism
Two views of counting mechanism, with (1) Scaler/Counter Meter and (2) Mask type worn during experiments shown at top. The bottom photo shows (1) Dolly, (2) GM Tube, and (3) Optical Bar with Slider.

in place. The dolly straddled the collection plate in the tray and was rigidly connected to an optical bar slider. The metric scale on the optical bar permitted precise, manual positioning of the dolly window along the plate. The scaler/count rate meter, Model DC-1900, was made by Nuclear Corporation of America.

Summary

This chapter has described the apparatus required for the current study. The theoretical portion was handled on an IBM 7094 Digital Computer. For the experimental portion, a closed-loop wind tunnel was used. Air in the tunnel was driven by a ventilating fan and passed through a three-plate electrostatic precipitator. The electric power required by the precipitator was provided by a high-voltage, DC rectifier. A micron-mesh, fiber glass filter was positioned aft of the precipitator to safeguard the fan and tunnel from the radioactive particles. The radioactive particles were commercially available 35 ± 5 and 7 ± 3 micron diameter microspheres containing the Scandium-46 isotope. The airstream velocity was measured by use of a hot-wire flowmeter while high-speed microphotographic cameras were employed to measure the particle velocities. The particles were injected into the airstream by compressed air after being loaded into the injection cylinder inside of a glove box. The procedures followed in working with the apparatus described above are given in the next chapter.

IV. Procedures

The procedures followed in solving the verification problem are detailed in this chapter. As in the case of the apparatus covered in the previous chapter, the procedures fell into the two broad, natural divisions of the problem, theoretical and experimental.

Theoretical

Stuart's digital computer program for solution of the electrostatic charging equation (Ref 8:App A) was the basis of a new IBM 7094 program, written to provide the theoretical predictions required in the present study. The program inputs were the operating parameters of the electrostatic precipitator and parameters of the particle. As output, the program provided the electrostatic charge acquired by the particle in the charging section and the point along the plate at which the particle would be deposited (referred to the plate front end). Complete details of the computer program, as well as sample input and output, are given in Appendix A. The theoretical results, or predictions, given in the next chapter are based on input data identical to the operating parameters of the experimental runs.

Experimental

The experimental procedures were dictated to a large extent by the hazardous materials involved in the study. However, the procedures, which were also directed towards attaining the study objectives, can conveniently be divided into three phases, i.e., preparatory, deposition run, and counting. The procedures for measuring the particle velocity

will be discussed separately. Although some of the safety precautions taken will be mentioned under the three phases noted above, the strong safety measures enforced throughout the test runs will appropriately be covered in a separate section.

Preparatory Phase. The preparatory phase, as implied, consisted of preparing the electrostatic precipitator to run and loading the injector mechanism. The first step was to cover the airstream side of the collector plates with aluminum foil, held on the plate by double-adhesive masking tape. No separation of the foil and plate was noted during any of the runs. The prepared plates and a clean filter were then placed in the precipitator and the doors sealed with heavy cloth masking tape.

The detachable injector cylinder, as previously mentioned, was loaded within a glove box in the radioactive storage room. Because the radioactive storage room and the equipment room were in separate buildings, the injector cylinder was always placed in a marked, sealed carton for transporting between buildings. Once the injector cylinder was placed in its position on the air line, the preparatory phase was complete.

Deposition Run. Procedures for the actual deposition run were rather simple and brief. After the fan was turned on and the airstream velocity stabilized, the high voltage supply was adjusted to the desired input voltage. (When deemed necessary, airstream velocity measurements were made prior to the high voltage being turned on.) The compressed air, flowing through the by-pass line, was then adjusted at the regulator to the desired flow rate and the upper petcock of the injector cylinder opened. After a last check of input voltage and compressed

air flow, the lower petcock of the injector cylinder was opened. Injection was almost instantaneous. A procedure reverse to the above was followed for shutdown.

Fourteen runs were made. As will be discussed under results, the runs were divided to ascertain the reproducibility of results as well as the effect that the variation of three parameters, (i.e., injection position, particle velocity, and applied voltage) would have on the precipitation pattern. The overall correlation between the experimental data and the theoretical predictions, made to establish the validity limits, was performed for all runs.

Counting Phase. Initial step in the counting phase was removal of the plates to the counting tray. The counting was accomplished using the GM tube and scaler activity counter described in Chapter III. The steel plates on the dolly were set into a .5 cm window and the dolly was advanced at .5 cm intervals until the count neared background activity. It was then advanced at 1 cm intervals, retaining the .5 cm window. Normally, two or three two-minute counts were made and the average used. The counts were curtailed to as low as .5 minute where high activity (5000-10000 cpm) warranted this action. The movement of the dolly and actuation of the counter was done manually, a rather long and tedious process. The counting procedure was in keeping with what Overman and Clark list as accepted practices in the field. With this procedure, the activity curves should have a standard deviation of no more than 3% at their peak values and no more than 6% at the lower levels of activity (Ref 7:114-122).

It is well to note here that, although the Scandium-46 isotope was selected on the basis of its gamma activity, it was its beta activity

that was used in the end. This is explained by the fact that with particles all of which have the same energy pattern, no energy discrimination was possible. By using the beta emission, the relative activity could still be plotted versus the plate length while the counting problem was somewhat simplified.

After the counting was completed, the aluminum foil was carefully removed from the plates by wrapping it on itself. As predicted from Baker's collection experiences (Ref 1:44-45), the particles adhered very strongly to the aluminum foil. There was no evidence (except in some early, heavy loadings) of any particles becoming detached from the aluminum foil. The wrapped foil was returned to the radioactive storage room and placed in the radioactive waste container for disposal according to local practice.

Particle Velocity Measurements. Several methods were considered for measuring the velocity of the particles, an item which proved rather difficult. Some of the methods considered included using the particle radioactivity with two separate counters, photoelectric cells, and phonograph needles. All were discarded because of the additional difficulties which would be generated by each of the methods suggested. The purpose behind all the methods proposed, however, was to mate the particle velocity to the airstream velocity at the ejection point.

The problem was finally solved to a certain extent by the use of high-speed microphotography. In this procedure, a millimeter scale was first photographed referenced to the nozzle end. The velocity was then determined by measuring the distance the particle traveled and the number of frames of film required for that travel. By also noting the

film timing marks, the velocity could be determined. Mathematically, this can be written as

$$\text{Velocity} = \frac{\text{Distance Traveled (cm)}}{\text{No. of frames}} \times \frac{\text{No. of frames/sec}}{\text{Timing Marks}} \times 1000$$

An actual example of the velocity measurement of a 7 $\pm$ 3 micron particle is

$$\text{Velocity} = \frac{.48 \text{ cm}}{7 \text{ frames}} \times \frac{82 \text{ frames/sec}}{7 \text{ timing marks}} \times 1000 = 804 \text{ cm/sec}$$

Safety. Because the radioactive materials and the high voltages were an integral and critical part of the experiment, this section is devoted to a compilation of the safety precautions observed during the experimental phases. Before receipt of the radioactive material, point source dose calculations were made on the basis of the calculated maximum amount that might be required per run, i.e., 0.5 gram. Shielding, or safe distance from source required, was also calculated. However, during the runs with the inert microspheres, it was learned that much smaller amounts of radioactive material would be required, i.e., about 0.1 gram or less. Even considered as point sources, this placed the dose in the low microcurie range, or approximately 5 microcuries.

Some of the physical precautions taken have already been mentioned, e.g., tape-sealing of the precipitator and filter access doors. In addition, all tunnel joints or equipment connections were sealed with gasket sealer material and covered with heavy, cloth masking tape. The injector cylinder was loaded with the radioactive material inside of a glove box to insure that none of the aerosol particles became airborne.

The injector cylinder as well as the rolled aluminum foil was transported between buildings in a marked sealed container. Laboratory smocks, rubber gloves, and face masks (Wilson, Model 809C, half-face masks (Fig. 11) were worn at all times that the radioactive material was being handled or in the room. Radiation hazard signs were also posted in conspicious places in the room and at the door.

To insure that current directives in handling of radioactive materials were complied with, all procedures were approved by the Air Force Institute of Technology member of the Wright-Patterson Air Force Base Radiological Health Hazards Committee. During the first "live" run with radioactive microspheres, a health physicist from the Radiological Committee observed and approved all procedures. The health physicist also performed wipe tests in and around the precipitator and injector cylinder areas.

The safety precautions taken for the high voltage required by the equipment began with the design of the precipitator. All resistors and connectors were placed under or behind the tunnel. Although open-end connectors were available on the door side for measuring of plate and grid voltages, all other connections and exposed wiring were away from positions where inadvertent contact could create a serious accident. Conspicious signs warning of the lethal nature of the voltage were also posted.

Summary

This chapter has described the procedures followed in solving the verification problem. The procedures, both theoretical and experimental, were aimed at establishing the overall correlation between the predicted

and actual precipitation patterns. The procedures were also aimed at determining the reproducibility of results as well as noting any effects caused on the precipitation pattern if the injection position, velocity, or applied voltage were varied. The deposition run procedures were divided into the preparatory, deposition run, and counting phases. The particle velocity was measured by use of high-speed microphotography. Safety considerations imposed by the hazardous nature of the materials and voltages involved were emphasized throughout the experimental phases. The results obtained with the procedures described is the subject of the next chapter.

V. Results and Analysis

General

The results obtained during this investigation are presented in this chapter and related to the study objectives in brief discussions under the respective objective heading. An analysis of the results is then presented, followed by a listing of the possible sources of the errors which exist between the experimental data and the theoretical predictions.

Fourteen experimental deposition runs were made. The theoretical and experimental results for these runs are presented in graph form (Figs. 12 - 25). Listed in Table I are the operating parameters for the electrostatic precipitator during each run. Also listed for each run is the theoretical deposition point of the primary-size particle (i.e., 35 in the 35±5 range). Before the results are discussed, however, the observations made from the high-speed microphotography should be noted.

Observations from High-Speed Microphotography

Several phenomena, considered highly significant to the results obtained, were observed in the three areas where high-speed microphotography was taken of the particle motion. The first area examined was in the vicinity of the nozzle during particle ejection. The differing velocities of the particles were distinctly noticeable in this area. Some particles could be seen overtaking and passing other particles, while others were observed with either an upward or downward velocity component. In other words, there was divergence, or spraying, in a small cone area at the nozzle. Particles could also be seen apparently colliding, with subsequent divergent vertical velocity components. The

Table I

Electrostatic Precipitator Operating Parameters with Ranges of Particle Velocities and Predicted Primary Deposition Area

Run	Particle Diameter (Micron)	Grid Voltage (KV/cm)	Collection Plate Volt. (KV/cm)	Corona Current (ma/grid)	Velocity Range (cm/sec) Range	Av	Primary Deposition x(cm)
1	35	9.3	7.50	1.460	(325-700)	450	1.1
2	35	9.3	7.50	1.460	(325-700)	450	1.1
3	7	9.3	7.55	1.465	(600-1100)	750	6.8
4	7	9.2	7.55	1.465	(600-1100)	750	7.0
5	7	9.2	7.55	1.475	(600-1100)	750	7.0
6	7	9.2	7.55	1.465	(600-1100)	750	7.0
7	7	9.2	7.55	1.465	(assumed)	950	8.8
8	7	9.2	7.55	1.465	(assumed)	950	8.8
9	7	9.2	7.55	1.465	(assumed)	950	8.8
10	35	9.2	7.55	1.475	(300-800)	650	1.7
11	35	7.3	5.60	0.475	(300-800)	650	3.0
12	7	7.2	5.55	0.475	(assumed)	950	16.2
13	35 7	7.3	5.60	0.475	(300-800) (assumed)	650 950	3.0 15.7
14	35 7	6.15	4.60	0.165	(300-800) (assumed)	650 950	5.1 28.2

NOTES:
1. Actual particle sizes are 35±5 and 7±3 microns.
2. Runs 1 - 10 were run at constant voltages and current. Small deviations noted are due to fluctuations in the readings.
3. Velocities for 7±3 micron particles at high flow rate are assumed. These particles could not be photographed with the available equipment at the high velocity.
4. All particles were injected into the lower channel at .475 cm below the charging grid.

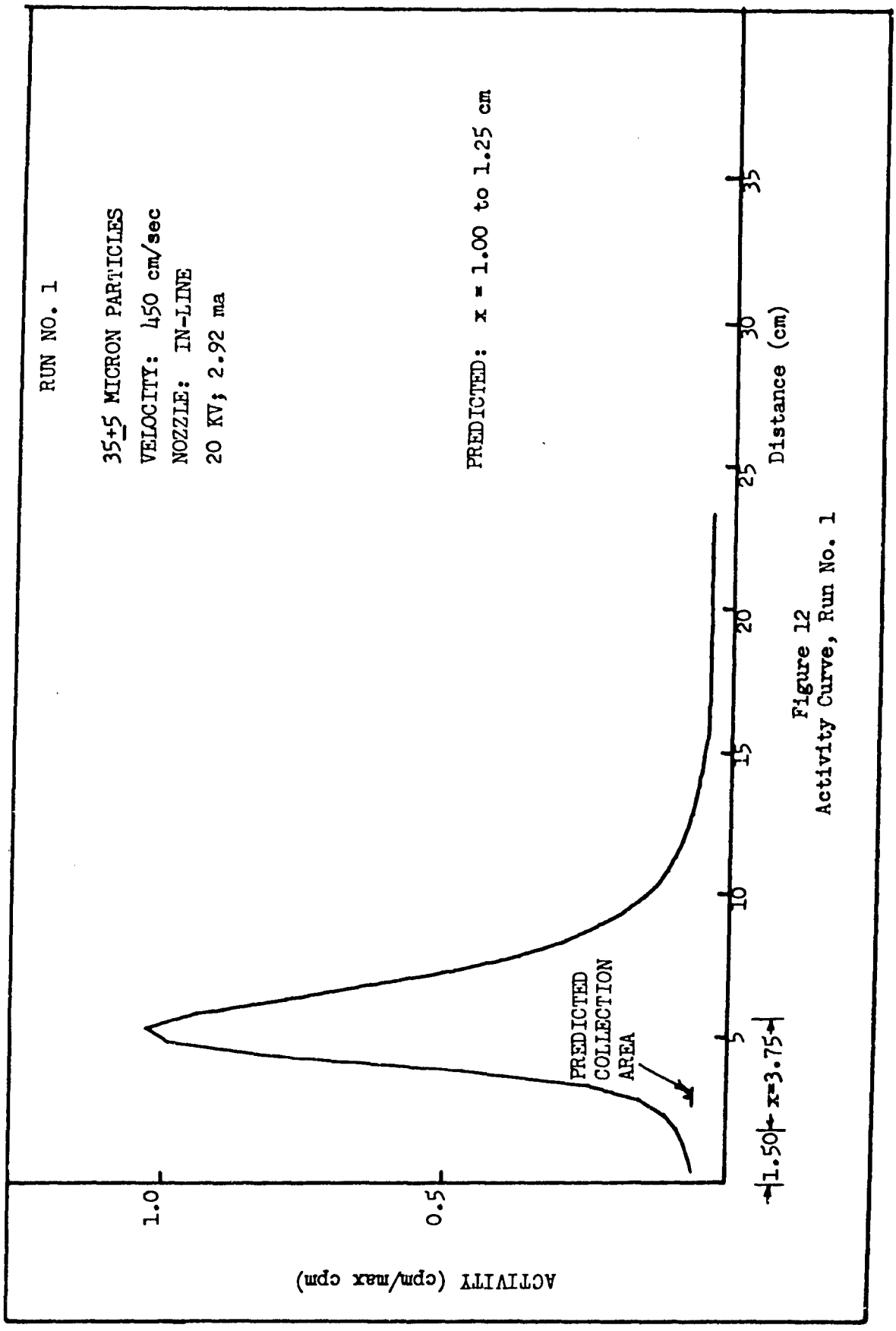

Figure 12
Activity Curve, Run No. 1

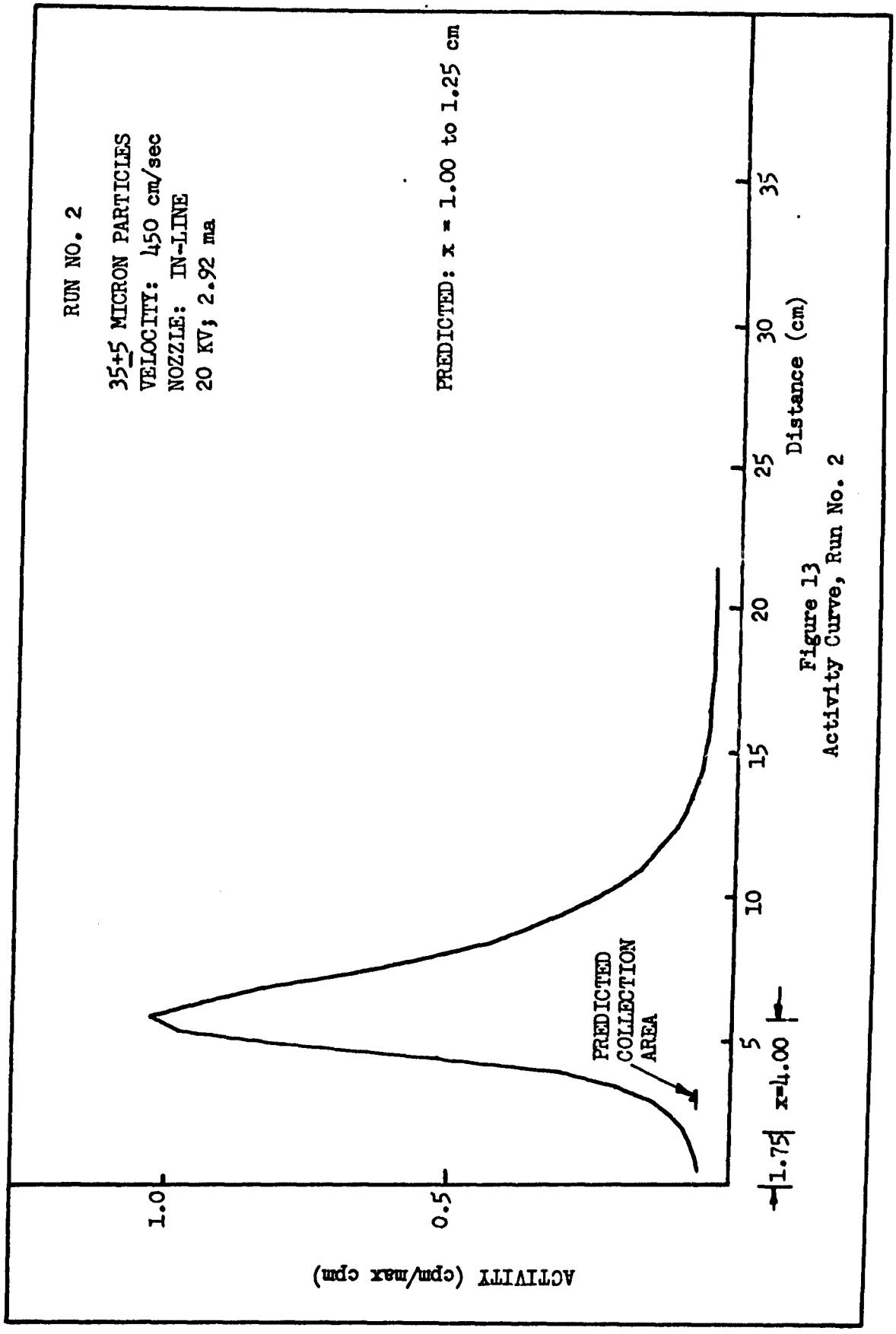

Figure 13
Activity Curve, Run No. 2

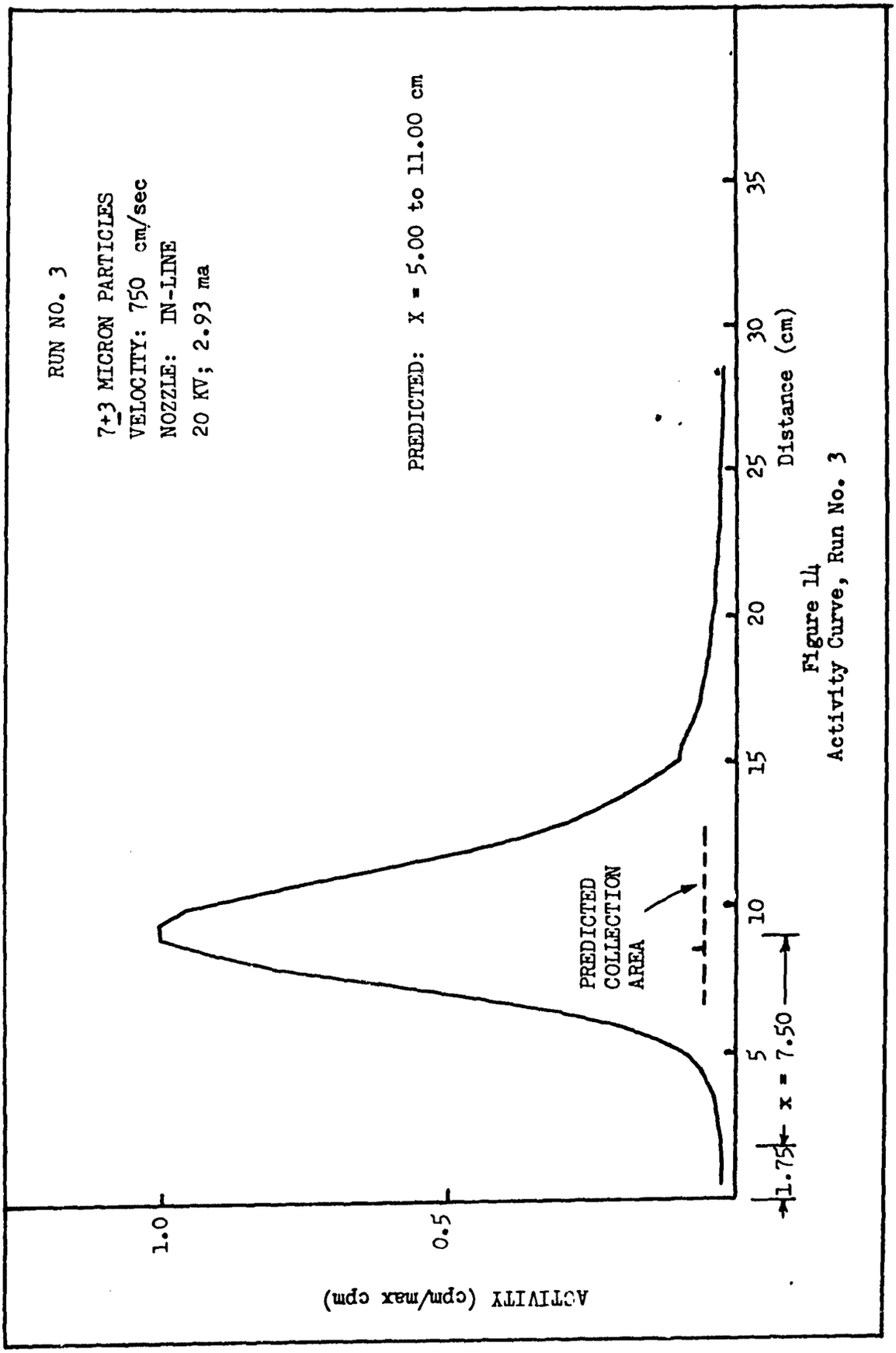

Figure 14
Activity Curve, Run No. 3

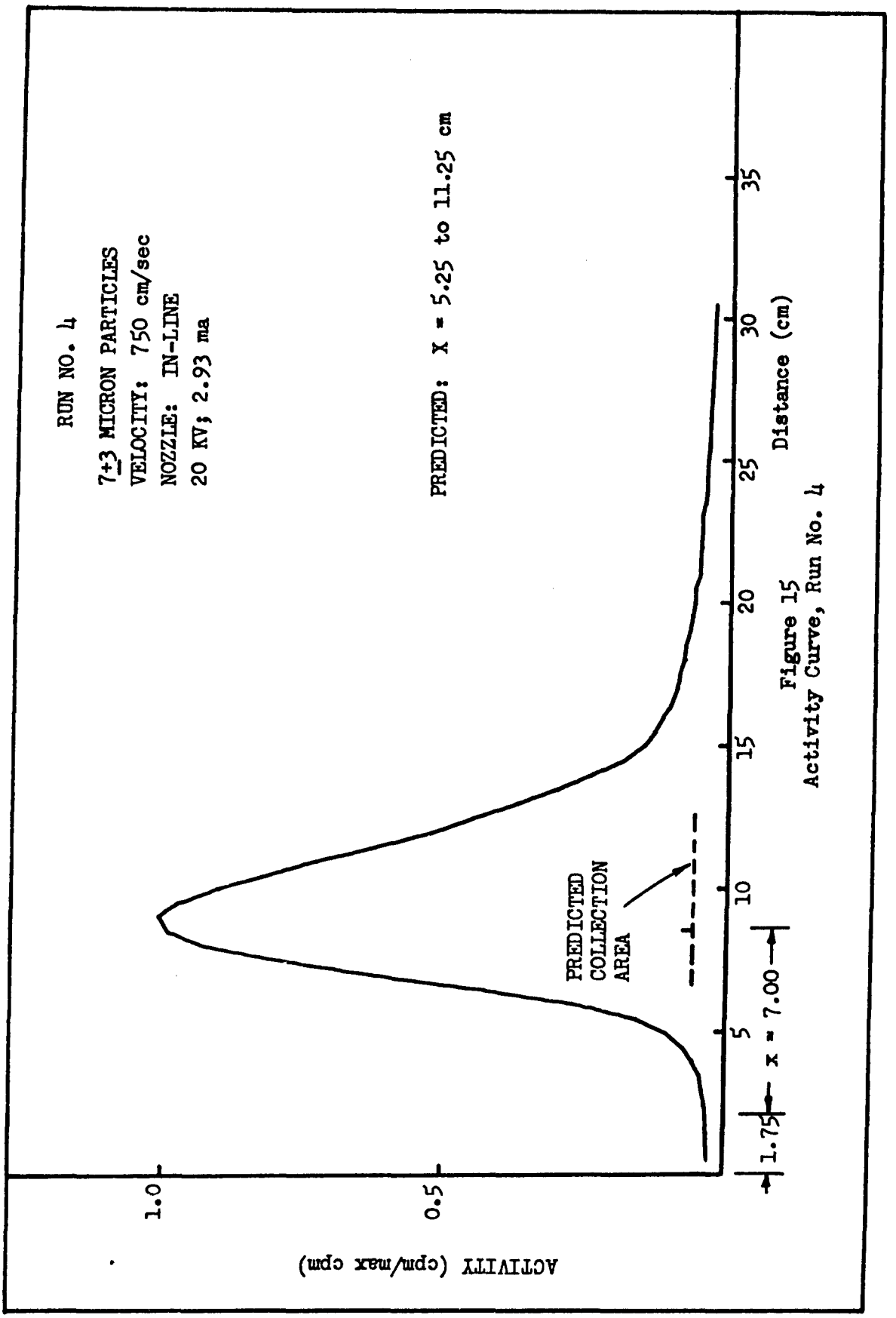

Figure 15
Activity Curve, Run No. 4

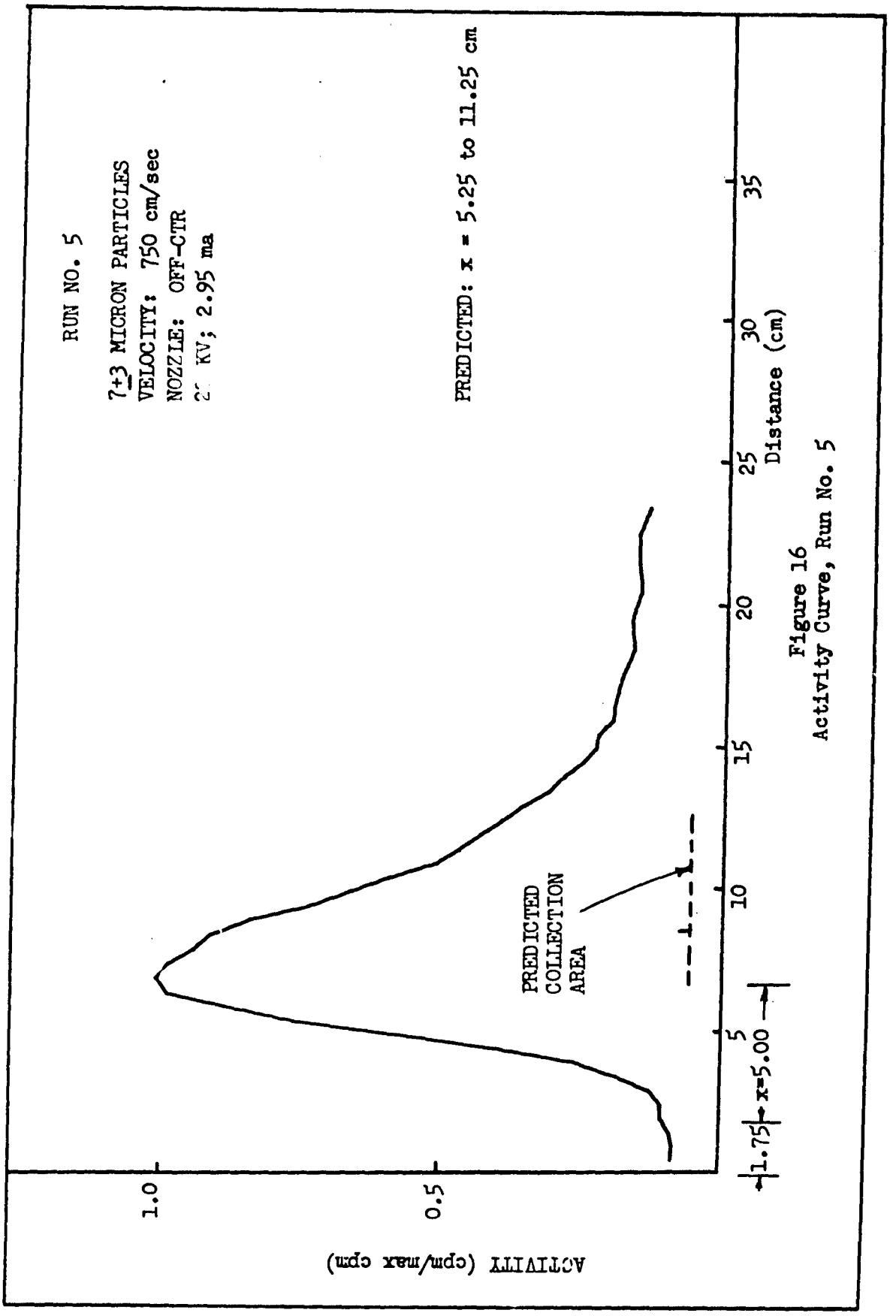

Figure 16
Activity Curve, Run No. 5

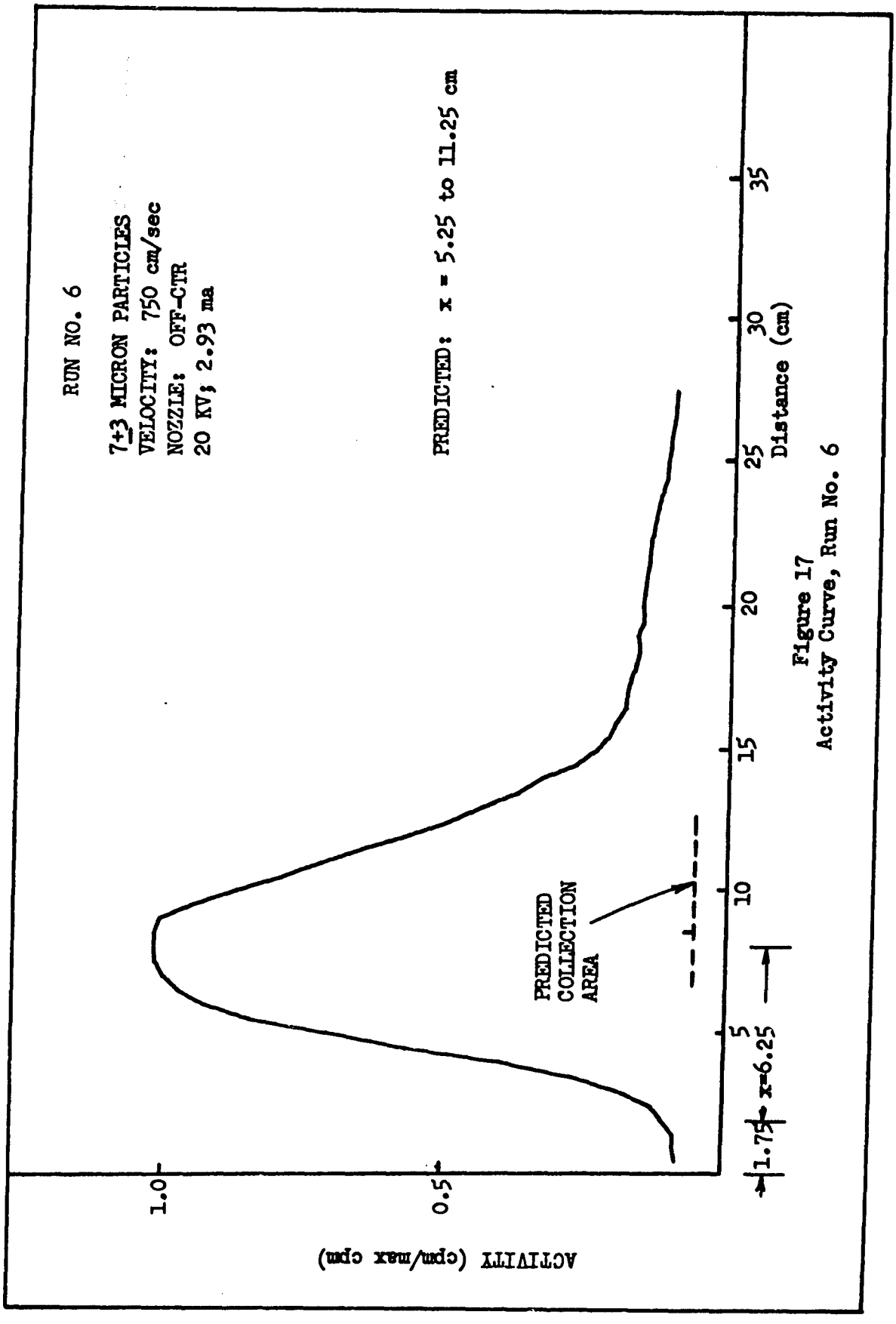

Figure 17
Activity Curve, Run No. 6

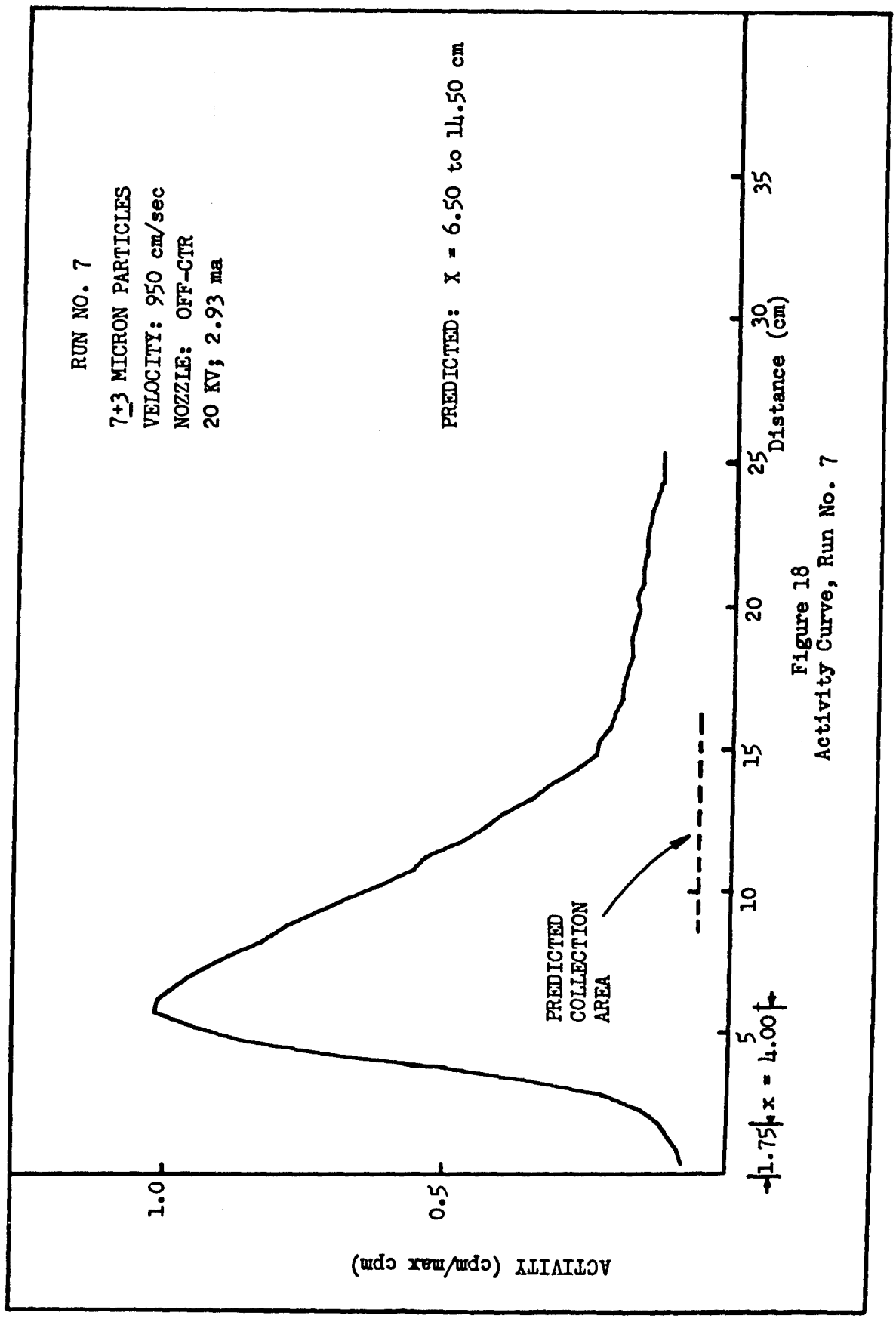

Figure 18
Activity Curve, Run No. 7

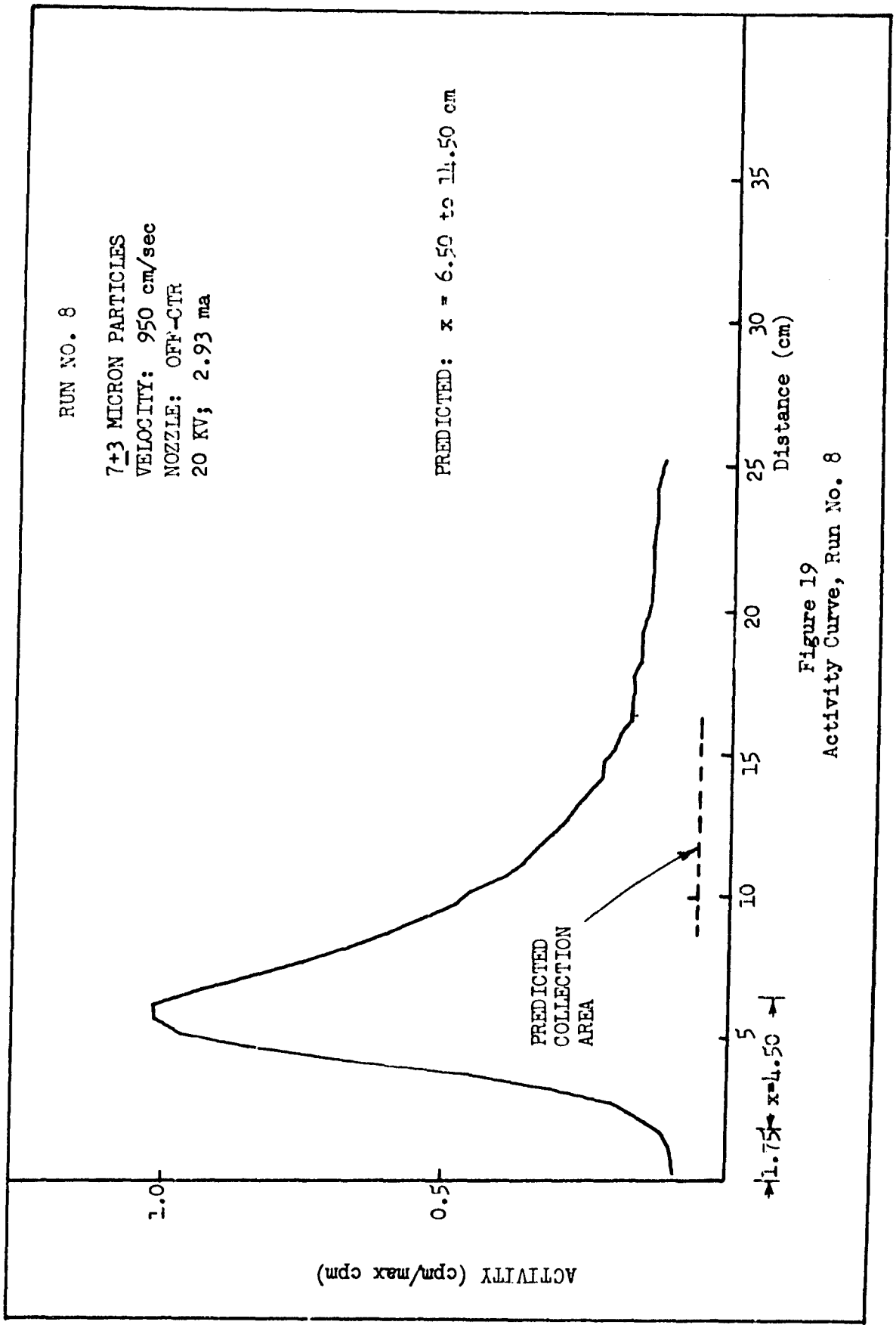

Figure 19
Activity Curve, Run No. 8

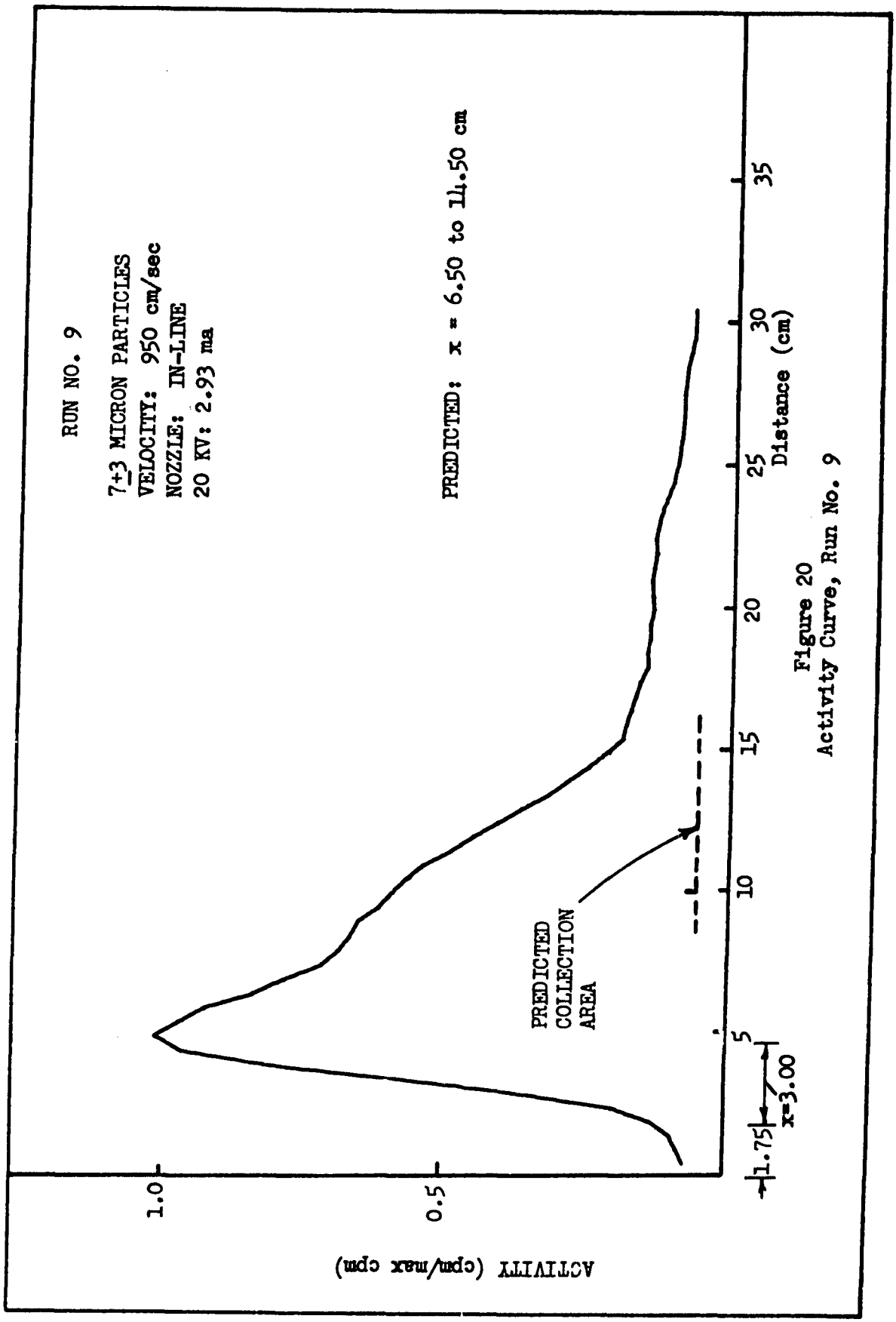

Figure 20
Activity Curve, Run No. 9

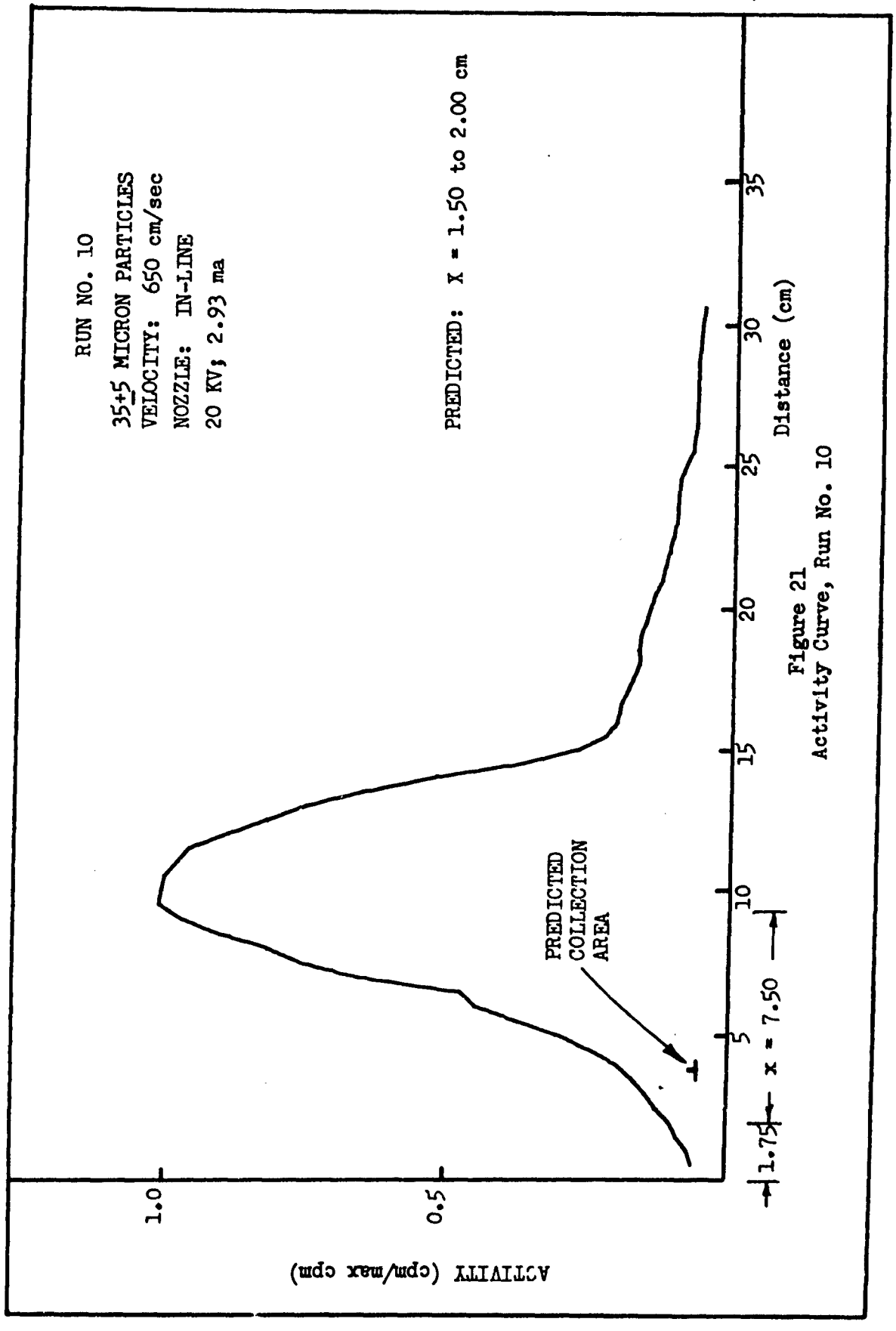

Figure 21
Activity Curve, Run No. 10

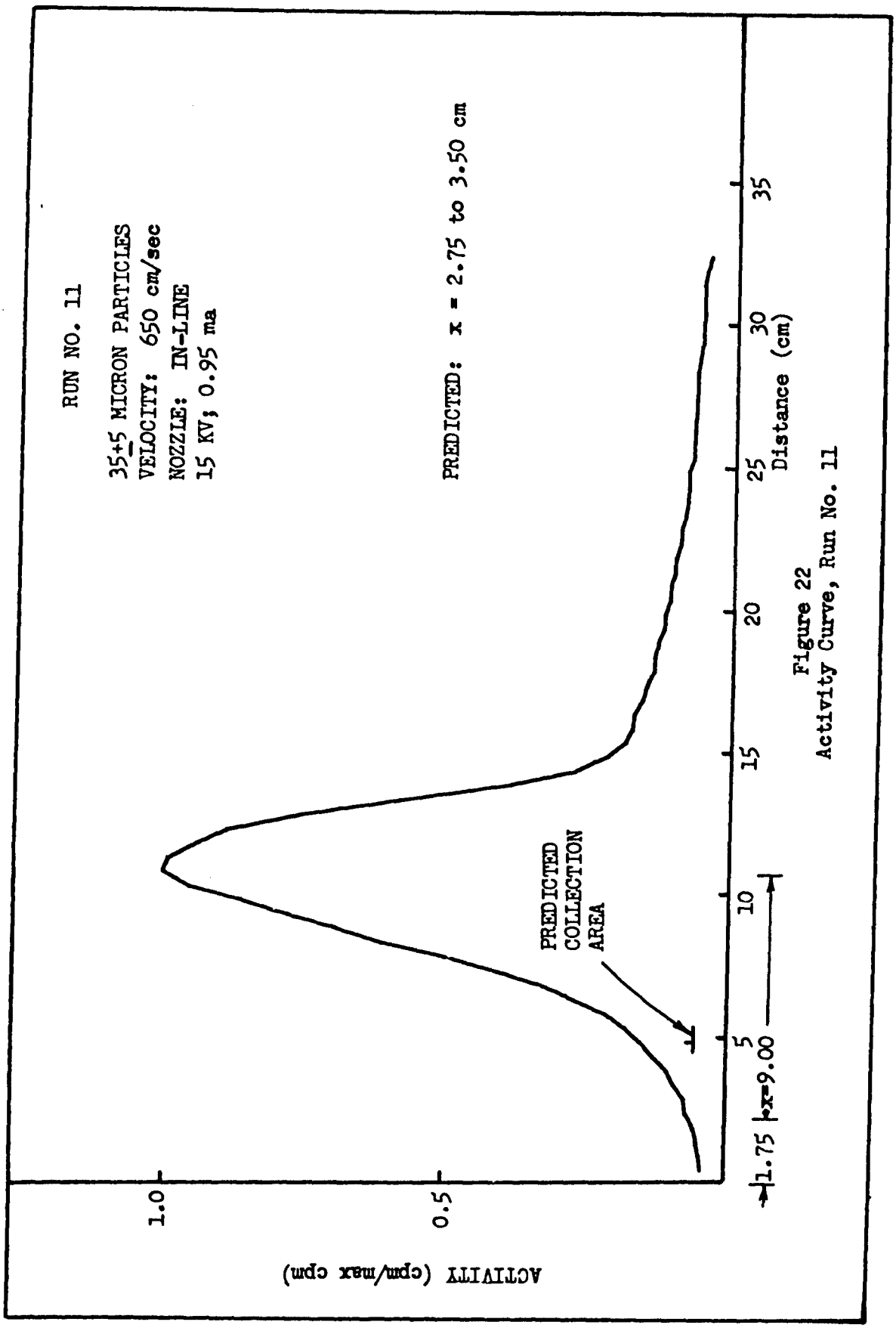

Figure 22
Activity Curve, Run No. 11

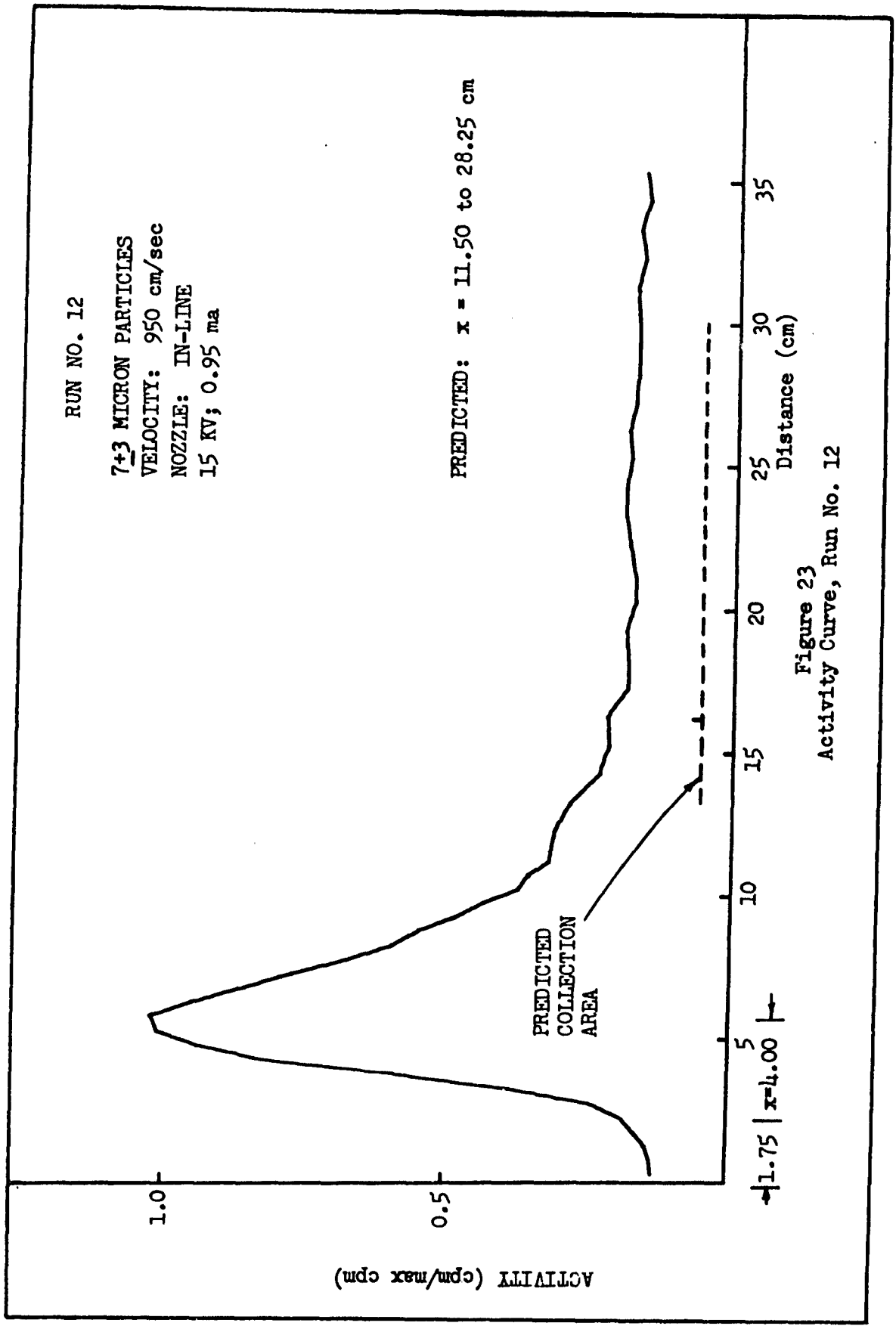

Figure 23
Activity Curve, Run No. 12

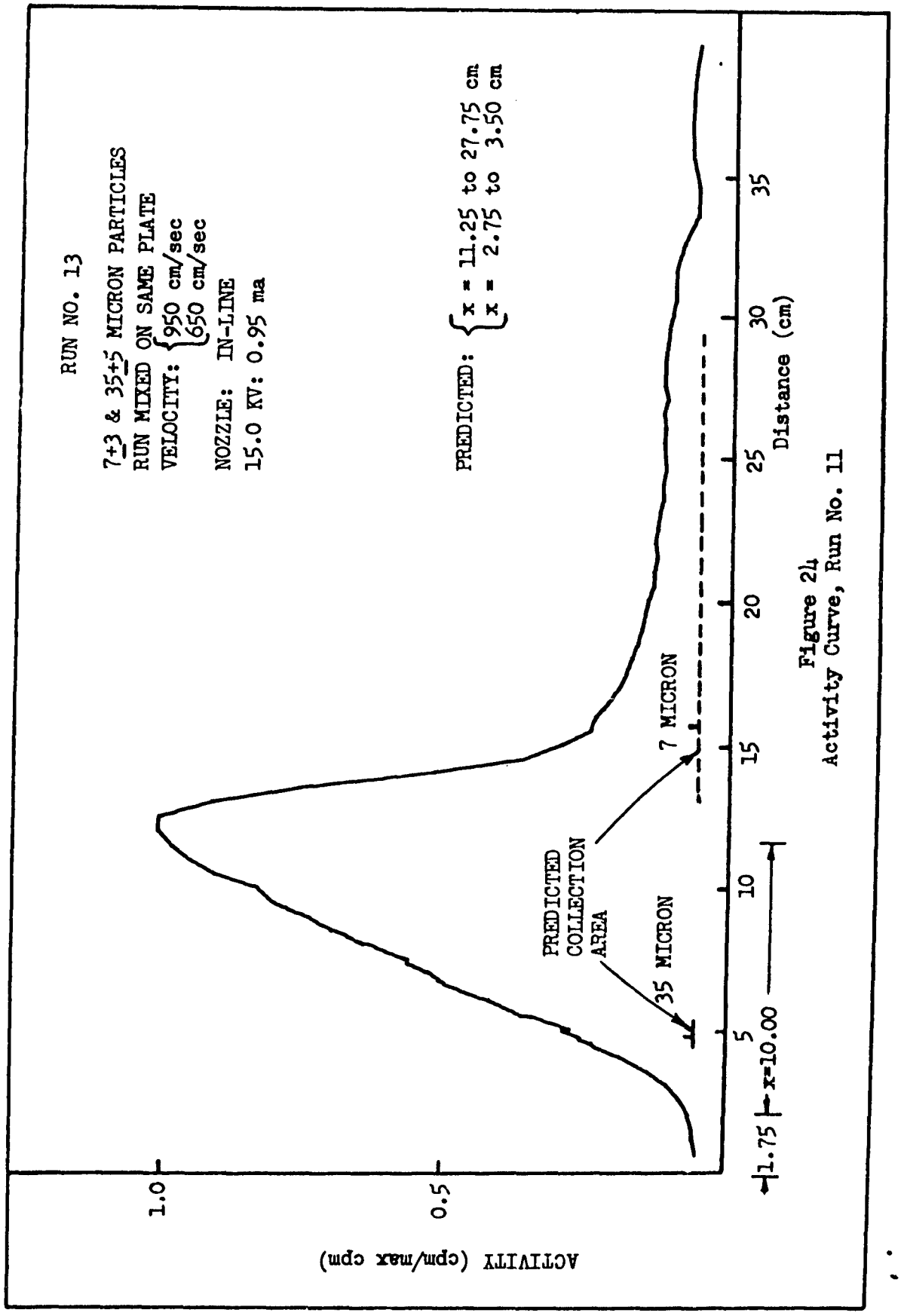

Figure 24
Activity Curve, Run No. 11

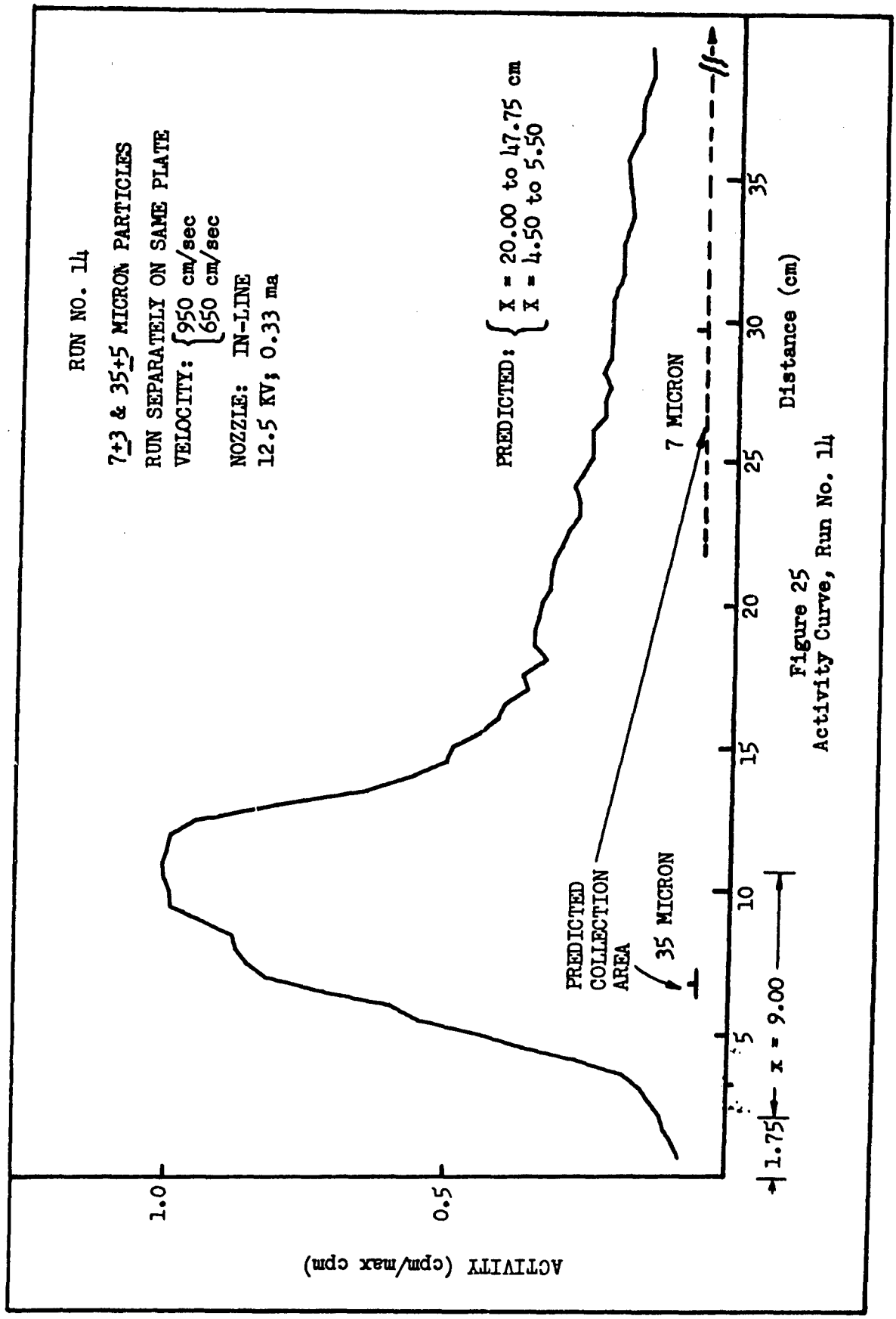

Figure 25
Activity Curve, Run No. 14

particles, for the most part, were ejected from the nozzle in a stream, grouped closely together.

The second area of observation was that of the particles entering the corona discharge section. In this area, the effect of the corona current and electrostatic field was clearly evident as the particles were accelerated in a downward direction. The particles were not as closely grouped in this area.

The deposition section of the collection plate was the last area photographed. The activity at this point is probably best described by a sequence of events. First, particles could be seen striking the plate and, in some cases, sliding along the plate. As more particles accumulated on the plate, a dense layer formed. As this layer was forming, a few particles could be seen bouncing slightly. As the layer became more dense, the particles bounced higher. In one case, a particle was seen to rebound three times in the camera field of view (approximately 8.5 mm).

The effect that the observed particle behavior might have had on the results is discussed in the Analysis of Results section. However, the differing velocities observed at the nozzle exit led directly to an average velocity being assumed for each particle group as explained below. The theoretical predictions are based on these assumed average velocities.

Theoretical Predictions

The theoretical predictions for the collection plate deposition areas are the results of the IBM 7094 Digital Computer Program described in Appendix A and are listed on the activity curve plot for each run. The area for the 35±5 micron particles is shown as a solid line; that for the 7±3 micron particles by a dashed line. The particle linear

velocity is one of the factors on which the theoretical predictions, as previously derived, are based. The range of the observed velocities for each run is given in Table I. (The two ranges for the 35±5 micron particles were measured with inert microspheres and assumed to remain the same for similar runs with radioactive microspheres. The measurements for the 7±3 micron particles were made, or attempted, in Runs 5, 7, and 8. The attempts, in Runs 7 and 8, to photograph the smaller particle at the high flow rate were unsuccessful due to insufficient resolution power of the available lens). Now, the particles also had a size distribution as shown in Table II for the 35±5 micron particles. It becomes apparent, then, that if the limits of the velocity range (both linear and vertical) are applied to the particle size extremes, a rather large and meaningless theoretical area of particle deposition will be obtained. However, if an average velocity were applied to the particle size distribution, the resulting theoretical deposition area should more nearly correspond to the real situation, where the larger particles travel slower than the small ones. The group as a whole, however, can be assumed to be traveling at an average velocity. Based on this reasoning, an average velocity was assumed (from observed values) for computing the theoretical predictions. The values are given in Table I. The predicted point of peak value, which is the deposition point of the primary size particle, is indicated on the graph by a small vertical line on the theoretical deposition line.

Experimental Results

The curves which depict the experimental results (Figs 12-25) are each normalized to the highest activity count for that run. The graphs were drawn with the Benson-Lehner Electroplotter Model J, using a 7094

Table II*

Size Distribution of 35±5 Micron Particles

Size (Micron)	Actual (Percent)
27.5	2
27.6 - 30.0	8
30.1 - 32.5	18
32.6 - 35.0	26
35.1 - 37.5	35
37.6 - 40.0	7
40.1 - 42.5	2
42.5	2
30 - 40	86

*Based on information in personal letter to the author from 3 M Company Nuclear Products Division

computer tape. The program for normalizing and plotting the curves is described in Appendix B. Also indicated on the graphs is the initial point of the "x" dimension, which was the beginning point of the corona discharge area. The initial point was normally 1.75 cm from the assumed point where the activity counting began. For further discussion, the results can be divided in light of the objectives given in Chapter II, i.e., overall comparison between experimental and theoretical data, reproducibility, and effects on the precipitation pattern caused by variation of injection position, particle velocity, and applied voltage.

Overall Theoretical vs. Experimental Results. A theoretical prediction was computed for every run and a comparison made with the experimental data. As can be seen from an examination of the graphs of all the results, deviation of the experimental from the theoretical ranges from good to poor. Runs 3 and 4 (Figs 14 and 15), made with the 7±3 micron particle at an assumed average velocity of 750 cm/sec, show extremely good correspondence between theoretical and experimental data. The correspondence for runs 5 - 10 (Figs 16-21), again made with the 7±3 micron particle but with different velocities, becomes worse as the velocity increases. The same description applies to Run 12 and the 7±3 micron portion of Runs 13 and 14 (Figs 24-25). In all the runs made with the 35±5 particles, the peak appears well downstream of the predicted deposition area, with the correlation worsening as the velocity increases. The correlation for the 7±3 micron particles also decreases but in the opposite direction, i.e. the experimental peak moves upstream as the theoretical moves downstream.

Reproducibility. The first four runs were made to determine if the experimental results could be duplicated from run to run if all precipitator operating parameters were held constant. Runs 1 and 2 (Figs 12-13) were made with the 35±5 micron particles. The curves have the same general appearance and the activity peaks are within 0.25 cm of each other. The shapes of the curves for Runs 3 and 4, made with the 7±3 micron particles, are essentially the same and the activity peaks are within 0.5 cm.

Variation of Injection Position. The next four runs, Runs 5-8 (Figs 15-18), were made with 7±3 micron particles and the injection position moved off-center. The particles were thus injected below and between the wires of the charging grid, rather than directly under the center grid wire. In addition to the off-center injection, Runs 7 and 8 were made at velocities of 950 cm/sec. The activity peaks of the first two curves have moved forward (upstream), while the latter two runs are slightly displaced in the downstream direction. The curves for all four runs appear fuller. Considerable activity was detected on the upper plate after these runs, contrasting markedly with the previous runs.

Variation of Particle Velocity. Runs 9 and 10 (Figs 20 and 21) were also made at 950 cm/sec to determine what effect a variation of velocity would have on the precipitation pattern. The 7±3 micron and 35±5 particles were used, respectively, in the runs. The activity peak for the 7±3 micron particles again appears to have moved upstream, while that for the 35±5 particle moved downstream. A certain amount of radioactivity was detected on the filter after all high velocity runs.

Variation of Applied Voltage. The remaining four runs (11-14, Figs 22-25) were made with a decreased applied voltage to determine the effect that this change would have on the precipitation pattern. Runs 13 and 14, in addition, were made with mixtures of the two size particles. In Run 13, the particles were mixed in the injection cylinder and injected simultaneously. In Run 14, each particle batch was injected separately. Although it was believed that two peaks might result, only one appears in both cases, each with a very slight dip in the forward slope near the top.

Analysis of Results

In general, the overall agreement obtained between the experimental and theoretical results was not very precise. Although at low velocities, correlation is excellent for the 7±3 micron particles (Runs 3-4) and fair for the 35±5 micron (Runs 1-2), the results seem to diverge as the velocity increases. The large particles seem to move downstream as predicted, but the small particles either move upstream or very slightly downstream (even though theory predicts considerable downstream movement). This is shown by a comparison of Run 11 with Run 10, both made with 35±5 micron particles, which shows an actual movement of 1.5 cm downstream as compared with a predicted 1.3 cm. The 7±3 micron particles, however, show considerable variance from theory when runs 12 and 9 are compared. The experimental displacement of Run 12 from Run 9 is only 1.0 cm as against a theoretical movement of 7.4 cm. Some of the possible sources of these errors in the correlation between the experimental and theoretical values will be discussed in the next section.

Nonetheless, the first four runs did demonstrate that under the same conditions and operating parameters, the results could be duplicated within experimental error. This result is extremely important if the theoretical model proposed by Lamberson is to be rigorously verified and applied in a practical manner.

Variation of the injection position in Runs 5-8 indicates that possibly the corona field was not uniform. The filling-in of the curve backslope and general flattening of the curve demonstrates that more particles could travel further when injected between the corona current grid wires than when injected in line with a grid wire.

The results of Run 9 indicate a complete deviation from the theory for the 7 ± 3 micron particle when the velocity is varied. This high velocity run should theoretically have an activity peak downstream of Run 3, its low velocity counterpart run. The opposite is true. On the other hand, Run 10, made with the 35 ± 5 micron particle, has its activity peak move downstream in the predicted manner when compared with Run 1.

The last four runs (11-14) demonstrate the effect that a variation of the applied voltage has on the precipitation pattern. In general, the activity peaks moved downstream as predicted, although the 7 ± 3 micron particle again moved much less than expected. The effort in the last two runs to separate the two different-sized particles by drastically reducing the applied voltage was not very successful. It appears that the wide range of the particle size distribution made the curves overlap into one continuous curve, rather than having two peaks as expected from Runs 11 and 12.

Possible Sources of Errors

There are several possible sources which may have contributed to the discrepancies noted between the experimental results and the theoretical predictions. The uncertainty in the velocity measurements, the method of particle injection and re-entrainment were undoubtedly the largest contributors to the errors noted. The method of particle injection, unfortunately, was not a true simulation of the collection of particles from an atmospheric aerosol. This source probably gave rise, or greatly contributed, to some of the other sources that will be described. Other sources are listed as possibilities although no attempt is made to evaluate the part that these others played in the error accumulation.

Velocity Measurements. The actual velocity measurements, carefully made from the high-speed microphotography, could contain some errors since the particles were photographed for a distance of less than 1 cm. Although an error analysis computation was considered for these velocity measurements, it was not performed. Assuming an average velocity for the particles in itself probably contains more and greater errors than could have been made in the measurements. Another, perhaps even greater, error may have been due to acceleration (or deceleration) of the particle group as a whole. No attempt was made (or considered possible) to determine whether the particles were undergoing any acceleration. However, any large acceleration (or deceleration) as the particles were ejected into a surrounding airstream of different velocity could have caused significant errors between the experimental and theoretical data. Some of the errors noted would be explained if the assumed velocity values were high for the 35 ± 5 micron particles and low for the 7 ± 3 micron particles.

Method of Particle Injection. The manner in which the particles were injected into the precipitator airstream resulted in a cloud-like, stream effect at the entrance to the corona discharge area. The particle velocities in this cloud-like stream were observed to vary rather widely. This is contrary to what one would expect in an airstream derived from the atmosphere, where particles are suspended and have reached a terminal velocity close to that of the airstream velocity. The velocity variance in a natural aerosol case could, therefore, be assumed to be much smaller.

The cloud effect also possibly negated the first two assumptions made by White in solving the particle charging equation discussed in Chapter II. Being in a cloud, the distance between particles was not much greater than particle diameter, as was originally assumed. Secondly, due to the field distortion caused by the particle proximity to one another, the corona field cannot be assumed to be uniform (White's second assumption). This effect, of course, would undoubtedly cause the particles to achieve a lesser charge which would lead to a lower transverse velocity and deposition farther downstream. This source of error would help explain some of the discrepancies noted for the 35 ± 5 micron particles, but not for the 7 ± 3 micron particles.

Re-entrainment. Re-entrainment is the re-introduction of a particle into the airstream after its initial deposition. Chiota (Ref 2:69-70), as well as White (Ref 11:1188), have discussed two possible causes of re-entrainment, i.e., erosion by the airstream and a layer of particles covering the anode. Although the second cause is known as "back corona" and should cause sparking during a run, no sparking was observed at any time during an experimental run. However, that there was considerable erosion by the airstream and that the layer of

microspheres covering the plate caused extensive re-entrainment was very apparent in the motion pictures. The downstream-side distortion of the activity curves is another indication of re-entrainment. One apparent explanation for the particles sliding along the plate (as seen in the high speed movies) may lie in the particle composition. Whereas a natural aerosol particle tends to flatten and literally "glue" itself to the collection plate, the ceramic microspheres, being spherical and hard, were attached over a small fraction of their surface, or literally, at a point. The particles could therefore be easily scraped off or dislodged, if desired. This contrasts markedly with Baker's experience of having to use ultrasonic cleaning (Ref 1:44) to remove the atmospheric aerosol particles that he collected.

Value of Dielectric Constant, K. Not knowing the value of the dielectric constant, K, of the particles also may have contributed to the errors seen between experimental and theoretical values of this study. By manipulating Lamberson's equations, Chiota illustrated the important role played by the dielectric constant in the expression for drift velocity. The equation derived was (Ref 2:63-64).

$$V = \frac{G\, E_1\, E_2\, r}{6}$$

for a given set of precipitator parameters, and where

V = Drift velocity (without Cunningham correction)

E_1 = Charging area voltage

E_2 = Collection area voltage

r = Particle radius

$G = 1 + \frac{2\,(K-1)}{K+2}$

It can be seen from the equation for G that substituting the theoretical value of K, or 4, into it makes G equal to 2. To see what effect a lower value of K would have on the theoretical predictions, a value of K=1 was substituted into the digital computer program. The results are shown in Table III. Examination of the table reveals that for K=1, the correlation between theoretical and experimental data is enhanced for the 35±5 micron particles, but a wider gap is created for the 7±3 micron particles.

Mathematical Models. The correlation between the experimental and theoretical data seems to diverge as the velocity increases and the particle size becomes smaller. This indicates that the mathematical models are imperfect. Three distinct areas exist which could cause the mathematical models to be in error.

In the original derivation of the theoretical model, Lamberson assumed "that the terminal velocity is achieved instantaneously upon interaction of the electrostatic force with the particle" (as it enters the charging section). Although admitting that the assumption was certainly not true, he argued that the time for the particle to achieve terminal velocity is small for the magnitude of forces and particle radii under consideration (Ref 6:51). The most favorable circumstance that Lamberson presents for the nearly complete charging of a 0.1 micron radius particle is 10^{-2} sec. (Ref 6:45). Stuart shows the charging curve for an 8.5 micron radius group, from which a charging time of .012 sec. can be read (Ref 8:29). This means that an 8.5 micron radius particle traveling 500 cm/sec would travel 6 cm; at 1000 cm/sec, the same particle would travel 12 cm. Some of the particles in this study were collected at less than 6 cm, indicating that they had probably not

Table III

Comparison of Theoretical Collection Areas (Based on Two Values of Dielectric Constant, K)

Avg Velocity (cm/sec)	Volt (KV)	Curr (MA)	35±5 Micron Particle						7±3 Micron Particle					
			Predicted Collection Area (cm)						Predicted Collection Area (cm)					
			40		35		30		10		7		4	
			K=4	K=1	K=4	K=1	K=4	K=1	K=4	K=1	K=4	K=1	K=4	K=1
450	20	2.92	1.0	1.8	1.1	2.0	1.3	2.2	3.1	5.6	4.1	7.6	6.6	12.5
600	20	2.93	1.4	2.7	1.6	3.1	1.7	3.4	4.1	8.8	5.6	11.8	9.0	21.1
700	20	2.93	1.6	2.3	1.8	2.6	2.0	2.9	4.8	7.5	6.4	10.1	10.3	17.6
750	20	2.92	1.7	2.9	1.9	3.3	2.2	3.7	5.1	9.4	6.8	12.7	11.0	22.8
950	20	2.93	2.2	3.8	2.5	4.2	2.8	4.8	6.6	12.1	8.8	17.2	14.5	30.3
650	15	0.95	2.7	4.6	3.0	5.1	3.4	5.7	7.7	14.2	10.3	20.5	17.4	36.2
950	15	0.95	3.99	6.7	4.4	7.4	4.9	8.4	11.3	22.8	15.7	32.3	27.7	56.1
650	12.5	0.33	4.6	7.5	5.1	8.2	5.6	9.2	12.3	24.7	17.2	34.8	29.8	59.9
950	12.5	0.33	6.8	10.9	7.4	12.0	8.2	13.7	20.1	39.8	28.0	55.7	47.8	95.2

NOTE: All distances rounded off to nearest tenth for this comparison

reached terminal velocity. In trying to determine the particle deposition areas with pinpoint accuracy, an acceleration distance of 6 to 12 cm would certainly cause errors in the estimate.

Another point in the original theoretical model is the fact that only the electrostatic and drag forces on the particle are considered. Although this is done on the basis of the assumption quoted above, the two-phase flow problem considered for the model does not appear quite that simple. Certainly the inertia forces in the 35±5 micron particles may have contributed to the data discrepancies seen in this study.

Lastly, the mathematical model derived in the present study for the computation of the theoretical collection area is also probably imperfect. In this model, the primary particle size and the two extremes of the known particle size distribution were used to obtain a linear theoretical area of distribution at deposition. However, the particle size distribution is not linear, or even normal. The distribution in Table II for the 35±5 micron particles is actually a triangular distribution, with the peak at about 37.5 cm and neglible amounts beyond that. It is now clear that a much more accurate theoretical model could probably be obtained if the particle size distribution and the particle specific activity were incorporated into the mathematical model.

Particle Composition and Size. Although both size particles were made of the same material, the larger particles (35±5 micron) gave the appearance of fine sand; the smaller, however, (7±3) tended to clump together. This could be explained by the higher surface tension of the smaller particle and the fact that these particles, according to the manufacturer, tend to pick up a layer of moisture. If this is, in

fact, true, the value of the dielectric constant (K) would be much higher than that assumed for the smaller particle. This would decrease the charging time and probably cause deposition of these particles sooner than predicted.

Turbulence. The last source of possible error is the turbulence of the airstream. The Reynolds number, which indicates the type of flow, is given by (Ref 3:131) as

$$R_e = \frac{VD}{\nu}$$

Where V is the mean velocity over the cross section, D is the hydraulic diameter and ν is the kinematic viscosity of the fluid in the test section. Evaluating for the precipitator collection section

$$D = \frac{4\ (\text{AREA})}{\text{Perimeter}} = \frac{\frac{4\ (.7874)\ (10)}{144}}{\frac{2\ (.7874)\ (10)}{12}} = .121 \text{ ft}$$

$$V = \frac{550 \text{ cm/sec}}{(2.54)\ 12 \text{ cm/ft}} = 18.05 \text{ ft/sec}$$

$$\nu = 16.88 \times 10^{-5} \frac{\text{ft}}{\text{sec}} \text{ for air at 1 atm, 80 F (Ref 3:504)}$$

and

$$Re = \frac{(18.05)(.121)}{16.88 \times 10^{-5}} = 1.295 \times 10^4$$

Since a Reynolds number above 3,000 usually indicates turbulence (Ref 3:131), it is assumed that the flow in the precipitator was turbulent. However, no attempt was made to estimate the error that turbulence may have caused.

Error Analysis

No formal attempt was made to establish limits of error for this study. As pointed out earlier, an average particle velocity was assumed for the computation of the theoretical predictions. An attempt to perform an error analysis on this assumption would be imprecise at best. The activity curves, based on the procedures used, should have a standard deviation of no more than 3% at their peak values and no more than 6% at the lower values of activity. Lastly, based on the 0.5 cm GM tube window and the 0.5 cm incremental measuring distance, the linear position (x distance) of the activity curve peak is assumed accurate to the closest 0.25 cm.

Summary

A summary and analysis of the fourteen runs made for the current study have been presented in this chapter. The correlation between the experimental data and the theoretical predictions runs from good to poor. The runs established excellent reproducibility of results and indicated that the precipitation pattern would change if particle injection position or velocity, or the applied voltage were varied. Possible sources of the errors noted between experimental and theoretical data are given and discussed. The main sources noted are velocity measurements, method of particle injection, and re-entrainment. Other possibilities given are the value of dielectric constant, particle composition and size, and turbulence. The conclusions that may be drawn from the results follow in the next chapter.

VI. Conclusions and Recommendations

The purpose of this thesis was to experimentally determine the limits of validity of the electrostatic precipitator theoretical model previously developed, in order that the model might be used in the design of a spectral collector. From the results summarized in the previous chapter, several conclusions may be made.

Conclusions

First, it can be stated without qualification that, with all parameters constant, the experimental results obtained are reproducible. Reproducibility of results is an extremely important criteria if the theoretical model is to be further developed into an air sampler, or spectral collector.

Secondly, the results clearly indicate that the phenomena which are occurring in the electrostatic precipitator can be described by mathematical models as suggested in the original theoretical approach. If the results are reproducible, then, certainly they should lend themselves to description by mathematical models.

Thirdly, the mathematical models so far derived are probably imperfect as they do not seem to accurately describe the particle behavior in the precipitator. Although good correlation appears to exist between the experimental data and the theoretical predictions at low velocities, the correlation seems to diverge as the particle size decreases and the velocity increases. In spite of the fact that the method of particle injection did not realistically simulate a natural aerosol, the divergence is too large and too consistent to disregard questioning the validity of the mathematical models.

Lastly, it can be concluded that, although a rigorous determination of the validity limits of the theoretical model was not achieved, enough correlation was found to exist between the experimental data and theory to indicate that investigation of the validity limits of the original theoretical model should be pursued.

Recommendations for Future Actions

The gains to be achieved by an electrostatic precipitator air sampler are quite large. Compared with today's methods of air sampling, where a small sample of air is analyzed over a long counting time, the benefits to be derived might even be termed "exciting". It is with these ideas in mind that the following areas are recommended for future study.

1. The experimental collection of data should be improved. Three areas of improvement that would lead to more realistic data are the injector mechanism, the motive power for the airstream, and corona grid geometry for a more uniform corona field. A six-prong rake or a conveyor-belt mechanism would make the injector mechanism more realistic, although it would probably require lining the wind tunnel to prevent contamination. To increase the velocities attainable in the wind tunnel, an air pump with greater pressure capacity is required. Improved geometry for the charging grid should continue to be investigated. One apparent approach would be to rig the charging grid wires perpendicular to the air flow direction rather than parallel as is now done.

2. A better method for velocity control and measurement should be sought. One method that could be adopted is a mechanical device, such as a Fermi Neutron-chopper, that would allow only one velocity group to be injected into the precipitator.
3. The mathematical models used should be carefully analyzed to insure their compatability with the actual phenomena occurring in the precipitator. Specific areas that should be investigated are the assumption in the original theoretical model that the terminal velocity is achieved instantaneously, the assumption to neglect inertia forces, and possible incorporation of the particle size distribution and radioactivity into the mathematical model.
4. More studies along the lines performed in this thesis should be conducted to further validate the theoretical basis of the electrostatic precipitator. Several other particle sizes (which are currently available from the manufacturer) in the 1 to 10 micron radius sizes should be tested.
5. The radioactivity counting process as used in this investigation should be automated. It should also be modified to scan the width of the plate at each station. Automating the process would allow more runs in that the counting could proceed virtually unattended. It would also allow the GM tube window to be made smaller to achieve greater discrimination.
6. An area which eventually will have to be investigated is the assumption by Lamberson that the radioactivity of natural aerosols is proportional to their size. Without validation of this portion of the theory, the entire concept would be on rather tenuous ground.

Bibliography

1. Baker, J. W. Sampling of Airborne Radioactive Particles by Electrostatic Precipitation. M.S. Thesis, Air Force Institute of Technology, 1962.

2. Chiota, A. J. Determination of the Size Distribution of Aerosols Collected by Electrostatic Precipitation. M.S. Thesis, Air Force Institute of Technology, 1963.

3. Eckert, E. R. G., and Drake, R. M., Jr. Heat and Mass Transfer. New York: McGraw-Hill Book Co., Inc., 1959.

4. Gelman Filtration Catalog: Sampling Equipment, Filters for Air, Gases and Liquids, Chemical-Medical Instruments. Chelsea, Michigan: Gelman Instrument Co., nd.

5. Lahr, T. N., and Ryan, J. P. Properties and Uses of a Unique Ceramic Carrier for Radioistopes. St. Paul, Minnesota: Nuclear Products Division, Minnesota Mining and Manufacturing Co., no date.

6. Lamberson, D. L. A Study of the Electrostatic Precipitation of Radioactive Aerosols. M.S. Thesis, Air Force Institute of Technology, 1961.

7. Overman, R. T., and Clark, H. M. Radioistope Techniques. New York: McGraw-Hill Book Co., Inc., 1960.

8. Stuart, R. S. The Analysis, Optimization and Design of an Airborne Radiation Sampling Electrostatic Precipitator. M.S. Thesis, Air Force Institute of Technology, 1962.

9. U.S. Department of Commerce, National Bureau of Standards. Handbook 69, Maximum Permissible Body Burdens and Maximum Permissible Concentrations of Radionuclides in Air and in Water for Occupational Exposure. Washington: GPO, June 1959.

10. U.S. Department of Health, Education, and Welfare, Public Health Service, Division of Radiological Health. Radiological Health Handbook. Washington: Office of Technical Services, U.S. Department of Commerce, September 1960.

11. White, H. J. "Particle Charging in Electrostatic Precipitation." Transactions: American Institute of Electrical Engineers - Part II, 70-1186-1191 (1951).

Appendix A

Precipitation Pattern Digital Computer Program

General

The IBM 7094 Digital Computer was used to make all the theoretical predictions found in this thesis. This appendix discusses the program through which the predictions were made and points out the reasoning behind some of the program steps. The program itself is based on Stuart's original computerization of the charging equation solution (Ref 8:App A). The List of Symbols and the Program Listing follow the program description, which is given next.

Description of Program

The purpose of the Precipitation Pattern Digital Computer Program is to predict the theoretical deposition point of micron-size particles in an electrostatic precipitator. The program uses the operating parameters of the electrostatic precipitator and the defining parameters of the particle as input data. As output, the program gives the charge acquired by the particle in the charging section as well as the particle deposition point along the plate, referenced to the front end of the corona discharge area. The program is designed to handle fifteen different-size particles combined with as many combinations of particle velocities and operating parameters of the electrostatic precipitator as required by the problem.

The charging problem is solved in the manner developed by Stuart (Ref 8:App A) and is completed by Statement 32. In Statement 32 the transverse velocity value in the charging section is described as a function of the varying charge. The same is done for the collection

section velocity in the Statement just above Statement 777. Note that in both of these equations a V0 term has been added. This allows incorporation of an initial vertical velocity value (either positive or negative) into the solution of the problem. Also note that C2 is the distance traveled due to gravity, or $\frac{1}{2}$ gt^2.

In solving the particle trajectory problem, the program takes DAC, the vertical distance that the particle has traveled, and combines it with the linear velocity to give X(J), the theoretical deposition point.

Two controls had to be incorporated into the program to prevent the exceeding of the vertical velocity dimension for small particles at high velocities. These controls, given by Statements 7 and 777, will complete the DO loop and allow the program to go to the next particle.

Input

The input data read-in is in two parts. The first one reads in the particle size (radius in centimeter) and the Cunningham Correction Factor as shown in the sample input. (Note: For the formula and values for the Cunningham Correction Factor, see Reference 6:72A-73). The next card or cards read-in the remaining variable values as given in Statement 31.

Output

The output (see sample) is in three parts. The first part is for identification purposes and is merely a print-out of the input variables as given in Statement 31. The second part is a Precipitation Pattern format with a statement for each particle size which gives its deposition position. The last part of the output is an incremental sequence of the amount of charge acquired by the particle during its passage through the charging section.

List of Symbols

Symbol	
AREA	Effective area of corona current discharge (cm^2).
CUN(J)	Cunningham Correction Factor for a particle (dimensionless).
COR	Corona current acting between the corona current grid and one plate (amps).
DAC	Distance traveled by a particle toward the anode plate (cm).
DCH	Length of the charging section (cm).
DELT	Incremental time change (sec).
DL	Length of collection section (cm).
E	Charging section ionization voltage (volts/cm).
ECOL	Collection section electrostatic field (volts/cm).
G	Ion density (ions/cm^3).
J	Particle size group (dimensionless).
IT	Fixed point value of TC below (sec).
QP	Time rate of change of charge $\frac{dq}{dt}$ (electrons/sec).
Q(J,I)	Charge at any time T. Becomes a constant as particle exits the charging section (electrons).
POS	Injection position of particle relative to the charging grid. Positive if below grid and negative if above (cm).
R(J)	Radius of a particle (cm).
RR(J)	The square of the particle radius, i.e., R(J)*R(J) (cm^2).
SEP	Plate separation between anode and cathode (cm).
TC	Time spent by the particle in the charging section (sec).
V(J,I)	Drift velocity at any time, TC, of a particle towards the anode. Becomes a constant when terminal velocity is achieved (cm/sec).
VO	Initial drift velocity of a particle as it enters the charging section. It is positive downward and negative upwards (cm/sec).

PRECIPITATION PATTERN
DIGITAL COMPUTER PROGRAM

```
CFERN ELECTROSTATIC PRECIPITATOR
      COMMON V,Q
      DIMENSION R(15),RR(15),G(15),H(15),A(15),B(15),C(15),
     1X(15),Q(15,750),V(15,750),CUN(15)
  100 FORMAT(15F4.0)
  101 FORMAT(24H1ERROR IN INPUT DATA, R(,I3,12H)IS NEGATIVE)
  102 FORMAT(6F10.0)
  106 FORMAT(1H1,F6.0,5X,F6.2,5X,F7.5,5X,F6.0,5X,F6.0,5X,
     1F8.6)
 1000 FORMAT(1HO,27HDIMENSION ON I GT THAN  749,2HC=E15.7,
     15X,2HV=E15.7)
 1001 FORMAT(1HO,27HDIMENSION ON I GT THAN  749,2HQ=E15.7,
     15X,2HV=E15.7)
  105 FORMAT(1HO5E20.8)
      PI = 3.1415927
      DELT = .0001
      DL = 62.4
      DCH = 12.7
      SEP = 2.
      AREA = 299.
      C1 = 1.602E-12/6./1.8E-04/PI
      C2 = .5*981.*DELT*DELT
      JN=0
    1 READ INPUT TAPE 2,100,R,CUN
      DO 2  J=1,15
      R(J) = R(J)*1.E-04
      IF (R(J))3,4,5
    3 WRITE OUTPUT TAPE 3,101,J
      GO TO 99
    5 JN = JN+1
      GO TO 2
    4 JN = JN
    2 CONTINUE
   31 READ INPUT TAPE 2,102,VL,VO,POS,E,ECOL,CUR
      DO 6 J=1,JN
      RR(J)=R(J)*R(J)
      G(J) =.352E19*CUR/E/AREA
      H(J) = RR(J)*G(J)*E
      A(J) = 11.16*H(J)
      B(J) = 14.406E-08*A(J)/E/RR(J)
    6 C(J) = B(J)*7.203E-08/2./E/RR(J)
      TC = DCH/VL
      IT = XFIXF(TC/DELT)
      DO 22 J=1,JN
      I=1
      DAC = 0.
      Q(J,I)=A(J)*DELT
```

```
      GO TO 32
    7 IF(I-749)500,500,999
  999 WRITE OUTPUT TAPE 3,1000,Q(I,J),V(I,J)
      GO TO 22
  500 QP = A(J)-B(J)*Q(J,I-1)+C(J)*Q(J,I-1)*Q(J,I-1)
      Q(J,I) = Q(J,I-1) + QP*DELT
   32 V(J,I) = VO + C1*Q(J,I)*CUN(J)*E/R(J)
   14 IF(POS)9,8,8
    8 DAC = DAC + V(J,I)*DELT+C2
      GO TO 10
    9 DAC = DAC + V(J,I)*DELT-C2
   10 IF(SEP-ABSF(POS)-DAC)20,20,11
   11 IF(IT-I)13,13,12
   12 I = I+1
      GO TO 7
   13 I = I+1
      Q(J,I) = Q(J,I-1)
      V(J,I) = VO + C1*Q(J,I)*CUN(J)*ECOL/R(J)
  777 IF(I-749)501,501,666
  501 GO TO 14
  666 WRITE OUTPUT TAPE 3,1001,Q(I,J),V(I,J)
      GO TO 22
   20 X(J)=VL*FLOATF(I)*DELT
      IF(J-1)23,21,23
   21 WRITE OUTPUT TAPE 3,103
   35 WRITE OUTPUT TAPE 3,106,VL,VO,POS,E,ECOL,CUR
  103 FORMAT(1HA,53X,21HPRECIPITATION PATTERN)
   23 WRITE OUTPUT TAPE 3,104,J,X(J)
  104 FORMAT(9HAPARTICLE,I3,20H WAS COLLECTED AT X=E15.8,4H
      DO 30 II =1,IT
      IF (Q(J,II)) 29,30,29
   29 WRITE OUTPUT TAPE 3,105,Q(J,II)
   30 CONTINUE
   22 CONTINUE
      GO TO 31
   99 CALL EXIT
      END
```

SAMPLE INPUT

```
20.0 17.5 15.0  5.0  3.5  2.0 (PARTICLE RADII)

1.0  1.0  1.0  1.02 1.04 1.06 (CUN CORR FACTOR)
```

VL	VO	POS	E	ECOL	CUR
450.	0.	.475	9300.	7500.	.001460

SAMPLE OUTPUT

PRECIPITATION PATTERN

```
450.      0.       .475      9300.     7500.     .001460

PARTICLE 1 WAS COLLECTED AT X = 0.10349999E 01 CM)

    0.76727045E 05      0.13234956E 06      0.20837025E 06
    0.23567384E 06      0.25835235E 06      0)27751531E 06
                          ETC.

PARTICLE 2 WAS COLLECTED AT X = 0.11250000E 01 CM.

    0.58744144E 05      0.10133013E 06      0.13382377E 06
    0.15953347E 06      0.18043779E 06      0.19780102E 06
                          ETC.
END
```

Appendix B

Activity Plot

Digital Computer Program

Purpose

The activity curves for all deposition runs were normalized and plotted through use of the IBM 7094 Digital Computer and the Benson-Lehner Electroplotter, Model J. The program described in this appendix enables the digital computer to normalize the activity readings for each run to the maximum activity reading for that particular run, and prepare a magnetic tape for plotter use. The tape is prepared through use of a prepared subroutine (Call Plot I), available at the Wright-Patterson Air Force Base Computer Facility. No attempt is made to describe the subroutine since it is available in self-explanatory handouts at the Computer Facility. In order to check the normalization, the input values as well as the corresponding normalized values are taken as output from the digital computer. A List of Symbols and the Program Listing are given after the Program Description which follows.

Program Description

The program listed herein is designed to read-in the activity values for each run and normalize them to the highest value for that run. The normalizing process is broken down into two sections, i.e., that where X (or abscissa) distance increases by 0.5 cm at a time and that where it increases by 1.0 cm. The first portion is given by statements 25 through 10; the second portion by statements from just below statement 10 to statement 20. The DO35 loop takes the normalized values and applies a scale factor to fit the plotting values to the scale selected in the plot subroutine.

The number of different curves plotted is controlled by Statement 15, with the value of KK initially being one less than the number of curves and negative. This control is necessary for the value of the LSR item in the "Call Plot 1" subroutine. The value of ISR must be one for the last time the subroutine is used and zero for all other times. The "If Statement" involving KK satisfies this requirement.

Input. The input to the program also consists of two sections, the control section and the activity values section. As seen below, the control section contains three variables, N, M, and DIV, which determine the abscissa (X) value for each corresponding normalized value of the activity (Y). In this case, N is the number of values, or readings, that are 0.5 cm apart, M is the total number of readings, and DIV is the maximum reading for that particular run. It should be noted that in the area (M-N) the readings are 1.0 cm apart. (The program was given this flexibility to correspond to the manner in which the experimental readings were taken). The Fortran II format for this input is given by Statement 101.

In the second input tape the activity values are read in consecutively, twelve values to a card. The Fortran II format for this input is given by Statement 100.

Output. The output from the computer run consists of the input values of X(I) and Z(I) (distance and activity) and the corresponding normalized value, Y(I). In addition, the output for plotter use, which has been recorded on magnetic tape, is given. The electroplotter then uses the magnetic tape to turn out graphs such as the Activity Curves, Figures 12-25.

List of Symbols

Symbol	
DIV	Value of the highest activity reading for a particular run. All other readings are normalized to this one.
KK	Number used to control value of LSR in subroutine. Its absolute value is one less than the number of curves (or plots). A negative number.
M	Total number of activity values.
N	Total number of activity values whose abscissa increment is 0.5 cm.
X(I)	Value of the variable which gives distance along horizontal axis (from left to right).
XX(J)	The value of X(I) corrected for scale factor.
Y(I)	Normalized value of the activity reading.
YY(J)	The value of Y(I) corrected for scale factor.
Z(I)	Input value of the activity readings.

ACTIVITY PLOT
DIGITAL COMPUTER PROGRAM

```
CFERN ACTIVITY PLOT
      DIMENSIONX(2000),Z(2000),Y(2000),XX(2000),YY(2000)
      KK=-13
 25   READINPUTTAPE2,101,N,M,DIV
      A=-.5
 101  FORMAT(2I5,F15.0)
  26  READINPUTTAPE2,100,(Z(I), I=1,M)
 100  FORMAT(12F6.0)
      DO10I=1,N
      Y(I)=Z(I)/DIV
      X(I)=A+.5
 10   A=X(I)
      NN=N+1
      DO20I=NN,M
      Y(I)=Z(I)/DIV
      X(I)=A+1.
 20   A=X(I)
      JJ=0
      DO185J=1,M
      IF(JJ)186,187,186
 187  WRITE OUTPUT TAPE 3,188
 188  FORMAT(4H1   X,6X,1HY,7X,1HZ,/1H )
 186  WRITE OUTPUT TAPE 3,189,X(J),Y(J),Z(J)
 189  FORMAT(1H ,F4.1,3X,F6.3,3X,F6.0)
      JJ=JJ+1
      IF(JJ-60)185,197,197
 197  JJ=JJ-60
 185  CONTINUE
      DO35J=1,M
      XX(J)=X(J)*(50.*20.00/40.)
 35   YY(J)=Y(J)*(50.*10.0)
 15   KK=KK+1
      IF(KK)30,30,40
 30   LSR=0
      GOTO41
 40   LSR=1
 41   CALLPLOT1(LSR,M,XX,YY,3,4,4,1,1,0,5,1.0)
      GOTO25
      END
```

SAMPLE INPUT

```
 N     M     DIV
45    46    30012.
```

ACTIVITY VALUES

```
  952. 1185. 1453. 1838. 2539. 3835. 6530.13171.22788.28879.
30012.27311.22592.18154.13686.10288. 7897. 6212. 4829. 3745.
 2922. 2388. 1974. 1601. 1370. 1116.  942.  766.  641.  532.
  436.  385.  341.  304.  290.  289.  280.  275.  250.  255.
  290.  279.  243.  230.  212.  197.
```

SAMPLE OUTPUT

X	Y	Z
0.	0.032	952.
0.5	0.039	1185.
1.0	0.048	1453.
1.5	0.061	1838.
2.0	0.085	2539.
2.5	0.128	3835.
3.0	0.218	6530.
3.5	0.439	13171.
	ETC.	

END